Discover Applied Sciences

Review

Incorporating sea sand into self-compacting concrete: a systematic review

B. M. Sindhurashmi[1] · Gopinatha Nayak[1] · N. D. Adesh[2] · Vidya Rao[3] · Sandhya Parasnath Dubey[3]

Received: 30 December 2023 / Accepted: 15 March 2024
Published online: 05 April 2024

Abstract
The increasing demand for river sand, driven by infrastructure development, poses environmental challenges. The study aims to address the depletion of river sand by integrating sea sand as a fine aggregate in the production of Self-Compacting Concrete (SCC) through a Systematic Literature Review. Furthermore, it includes an in-depth bibliographic analysis of relevant literature using VOSviewer to generate network visualizations of author-co-citation and country-wise citations. The article offers diverse options for sustainable solutions to mitigate environmental impacts while meeting infrastructure demands. It focuses on assessing the durability of SCC incorporating sea sand through real-time monitoring with the Internet of Things (IoT) and employing artificial intelligence methods like PointRend and neural networks to study the properties of SCC utilizing sea sand. Subsequently, the study emphasizes the need to address river sand shortages in infrastructure development and provides insights for further research on enhancing the properties of SCC with sea sand.

Article highlights

- A Systematic Literature Review (SLR), coupled with a bibliographic analysis using VOSviewer.
- Concrete incorporating non-desalted sea sand showed lower porosity and sorptivity compared to desalted sea sand, due to matrix densification from Friedel's salt.
- Integration of Internet of Things (IoT) and artificial intelligence methods like PointRend and neural networks are vital for analyzing the properties of SCC with sea sand.

Keywords Self-Compacting Concrete (SCC) · Sea sand and river sand · Internet of Things (IoT) · VOSviewer · Supplementary Cementitious Materials (SCMs) · Artificial Intelligence (AI) · Systematic Literature Review (SLR)

✉ Gopinatha Nayak, nayak.gopinath@manipal.edu; B. M. Sindhurashmi, sindhurashmi.bm@gmail.com | [1]Present Address: Department of Civil Engineering, Manipal Institute of Technology, Manipal Academy of Higher Education, Manipal, Karnataka 576104, India. [2]Department of Information and Communication Technology, Manipal Institute of Technology, Manipal Academy of Higher Education, Manipal, Karnataka 576104, India. [3]Department of Data Science and Computer Applications, Manipal Institute of Technology, Manipal Academy of Higher Education, Manipal, Karnataka 576104, India.

(a) In Dibamba River, Cameroon, people were digging river sand

(b) In Tanzania, riverbeds are eroded as a result of excessive river sand extraction

Fig. 1 Adverse effects caused by excessive river sand mining [5, 6]

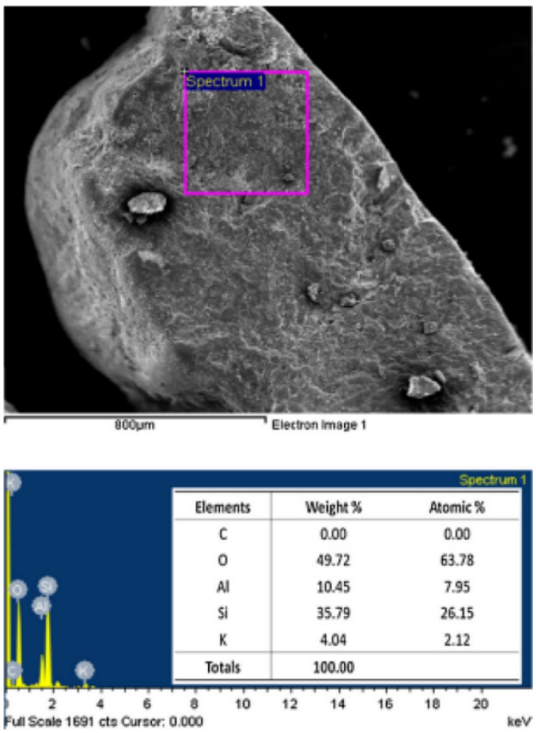

Fig. 2 Findings of the EDX test conducted on RS [11]

1 Introduction

Recent innovations conducted by a plethora of researchers in the construction industry have intensified global interest in sustainability [1, 2]. The scarcity of river sand adversely affected the natural environment and has also increased the price of river sand [3, 4]. The increased mining of river sand results in a shift in the river's flow pattern, resulting in the formation of a new catchment area. This change has the potential to result in flooding. These alterations could have a negative impact on the river's ability to convey water, altering the overall hydrological equilibrium [5].

The Fig. 1 illustrates the adverse effects caused by excessive river sand mining [5, 6]. Figure 1a shows people digging river sand in the Dibamba River, Cameroon. Figure 1b shows the erosion of riverbeds caused by the excessive mining of River Sand (RS) in Tanzania. This problem has motivated researchers to undertake further investigations into the utilization of seawater [7, 8] and Sea Sand (SS) in concrete [9, 10].

An Energy Dispersive X-ray (EDX) test result demonstrated in the Fig. 2 shows that River Sand (RS) particles were free of chloride, as evidenced by the test result of the elemental analysis. Figure 3 illustrates the findings of the EDX

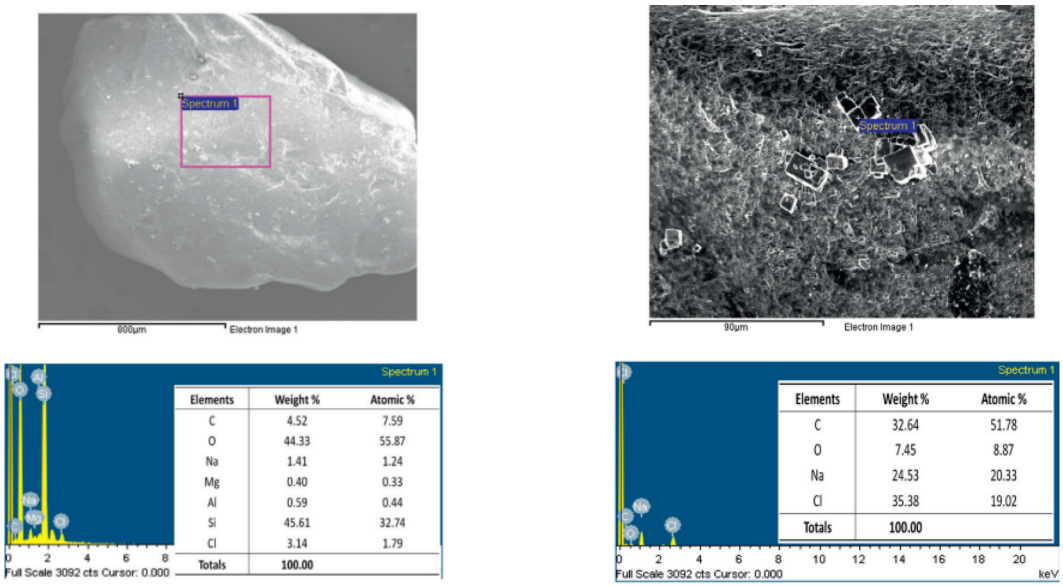

(a) Elements found in the square region of the surface of the DMS

(b) Presence of elements at a specific point on the surface of the DMS

Fig. 3 The results of the EDX test carried out on DMS [11]

examination conducted on Dredged Marine Sand (DMS). Figure 3a visually indicates the presence of chloride ions within the DMS, indicating a possible contributing factor to the degradation of steel bars. According to the elemental analysis, the chloride concentration was 3.14% by weight [11]. Figure 3b illustrates an enlarged microstructure from the highlighted area in Fig. 3a, presenting the EDX test findings for crystal materials affixed to the DMS surface. Examination of the elements disclosed in these EDX results suggests the identification of the cubic crystals as NaCl.

In the study [14], it was discovered that sea sand (zone 3) exhibited greater fineness in comparison to river sand. Table 1, and Table 2 summarizes the physical properties of sea sand. The Fig. 4 illustrates the particle size distribution for both Sea Sand (SS) and River Sand (RS).

In comparison to river sand, sea sand showed smaller particles, as indicated by its fineness modulus of 2.49, whereas river sand showed a higher fineness modulus of 2.84 [12]. Studying seashell properties becomes essential, particularly given the presence of seashells in sea sand. Seashell fragments, mostly smaller than 1 mm, contribute to seashells with dimensions less than the bulk sea sand. They exhibit an average diameter of 0.747 mm and a most frequent diameter of 0.52 mm, illustrating a left-skewed distribution, as depicted in Fig. 5. Additionally, the investigation [18, 19] revealed the irregular texture of the sea sand. An examination of chemical components (%) of river sand and sea sand is displayed in

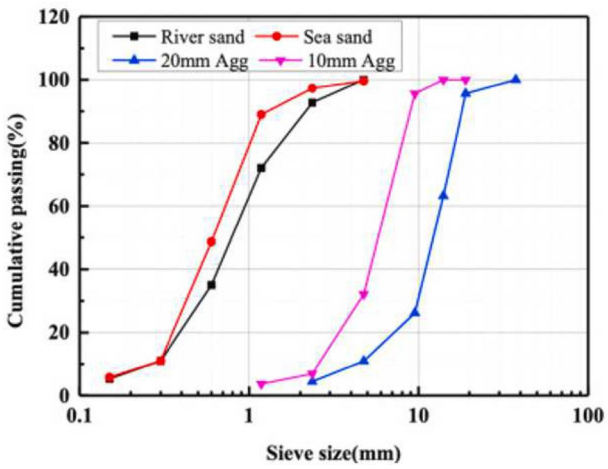

Fig. 4 Particle size distribution of SS and RS [12]

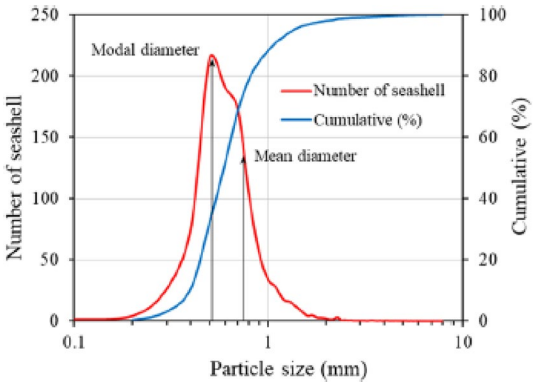

Fig. 5 Particle size distribution of seashells [13]

Table 1 Physical properties of the sea sand [15]

Sl. no.	Properties	Unit	China (desalted)	Neilingding Island	Daya Bay of Huizhou	Pearl River Estuary
1	Shell content	%	0.29	0.78	0.88	1.12
2	Fineness modulus	–	2.85	3.03	–	–
3	Bulk density	kg/m^3	1415	1490	1450	1475
4	Sediment content	%	0.88	1.29	1.36	1.02
5	Apparent Density	kg/m^3	2618	2625	2578	2661
5	Tight density	kg/m^3	2015	2095	2055	2072
6	Water content	%	4.35	4.89	4.85	4.85
7	SO_3 /SO_4^{2-}	%	0.37	0.42	0.54	0.47
8	Ruggedness	%	2.96	2.83	3.28	3.38

Table 2 Properties of the sea sand [16, 17]

Sl. no.	Properties	Unit	Place	Value
1	Oven dry specific gravity	–	Indonesia [16] Coimbatore [17], India	2.43 [16] 2.71 [17]
2	Saturated surface dry specific gravity	–	Indonesia [16]	2.47
3	Water absorption	%	Indonesia [16]	1.75

Table 3. The chloride content in non-desalted sea sand was determined to be 0.1968%, whereas in desalted sea sand, it was found to be 0.0090% [20]. Researchers have provided solutions by conducting simulated rain tests, water washing [21], hot water washing for the sea sand to scale down the chlorine content [22] in the sea sand. Water washed sea sand and hot water washed sea sand have shown permissible chloride content (less than 0.05%). Additionally, researchers examined strategies to improve the anti-corrosion characteristics of marine concrete by incorporating Layered Double Hydroxides (LDHs) and Polyvinylpyrrolidone (PVP). These substances exhibited significant anti-corrosion effectiveness, indicating considerable promise as effective inhibitors for preventing corrosion in marine concrete. The rapid chloride migration coefficient showed a reduction of 17.5% compared to the control group, and the total charge passed decreased by 4.9% according to the study [23]. Therefore, in island construction, Seawater Sea Sand SCC (SWSS-SCC) has more environmental benefits than when used in coastal buildings [24]. Additionally, the assessment of the physical characteristics of the Non-Treated Sea Sand (NSS) and Desalted Sea Sand (DSS) obtained from Karatsu harbour of Saga Prefecture, Japan are as shown in Table 4.

According to the Chinese Code of the Ministry of Construction of the People's Republic of China, the chloride ion concentration in dry sand should not exceed 0.06% for reinforced concrete and should be limited to 0.02% for pre-cast reinforced concrete respectively [28–31]. The US code of the American Concrete Institute (ACI) specifies less than 0.06% of chloride to the weight of concrete. Furthermore, ACI also provides a clear indication that the chloride ion should be

Table 3 Comparison of chemical components of river sand and sea sand sourced from Nagore, Tamil Nadu, India (%) [25]

Elements	River Sand	Raw sea sand	Sea sand after simulated rain test	Water washed sea sand	Hot water washed sea sand
C	5.03	11.05	10.50	12.61	12.48
Si	58.09	53.00	51.08	54.29	47.13
O	21.61	32.57	33.80	29.88	39.26
Mg	0.42	0.12, 1.1 [16]	0.28	0.10	–
Al	7.80	1.24, 12 [16]	1.78	1.47	0.76
K	5.05	–	–	–	–
Fe	0.91	0.57, 3.6 [16]	1.34	1.58	0.30
Na	1.09	1.36	1.14	0.05	0.04
Cl	0.00	0.09 [26] 0.04 [16] 0.026 [27] 0.03 [15] 0.1968 [20]	0.08	0.02, 0.0054 [20]	0.03

lower than 0.08% and 0.15% of the mass of the concrete in wet and dry conditions for reinforced concrete. The Japan Architectural Standard specification specifies that sea sand must have a chloride ion content lower than 0.04% by mass of the dry sand or less than 0.3 kg/m^3 in the concrete [20]. IS 456: 2000 (Reaffirmed: 2021) specifies that the acid-soluble chloride content of reinforced concrete or plain concrete with metal should be lower than 0.6 kg/m^3 [32, 33]. Allowable ranges for the characteristics of sea sand as per JGJ 206–2010 [15, 34] are as shown in Table 5.

According to IS 650:1991 (Reaffirmed: 2018) [35], the standard sand must be quartz, light grey or whitish, and silt-free. Its grains should be angular and mostly spherical, with minimal presence of elongated and flattened grains. Additionally, the standard sand must pass through a 2 mm IS sieve completely and remain on a 90 micron IS sieve, demonstrating the particle size distribution outlined in Table 6. Moreover, as per IS 383:2016, seashore gravels and seashore sand are naturally rounded in shape. The permissible limits of harmful substances in fine aggregates, as specified by IS 383:2016 are presented in Table 7.

The research community has consistently been striving to reduce the number of workers needed for construction. However, in this context, it is necessary to modify construction practices to cut down on the utilisation of river sand [37, 38], construction time, and labour force by using innovative concrete. Many advancements within the construction sector have been documented over the recent years [39–41]. From the aforementioned studies, it is possible to utilize sea sand in the production of SCC. SCC was implemented in Japan by Okamura and Ozawa in the year 1989 [32]. SCC is an innovative state of the art type of concrete that would be compacted through its own weight, terminating the need for mechanical vibrators [42]. Well-graded materials, superplasticizers are used in the production of SCC [42]. Eliminating vibrating equipment will help the construction site workers by reducing noise and vibration. Using SCC at a construction site will enhance health and safety benefits, as well as improve efficiency, for both pre-cast concrete and various other constructions [42, 43].

Extensive substitution of sea sand for traditional fine aggregate in SCC production is restricted owing to its susceptibility to chloride-induced steel corrosion [44, 45]. However, researchers have explored alternative solutions, such as the use of mineral admixtures [46, 47] and Fiber Reinforced Polymer (FRP) [48–50] reinforcement, textile reinforcements, and Aluminium Metal Matrix Composites (AMMCs) to resolve the structure's durability issue [51, 52]. FRP jackets/tubes employed for concrete columns are manufactured by using Glass FRP (GFRP) [53–55], Aramid FRP (AFRP), Polyethylene Terephthalate (PET) FRP [56], and Carbon FRP (CFRP) [57, 58]. Concrete made by using FRP [59] acts as more ductile when compared with conventional concrete [60]. Although colossal investigations are happening in the field of SCC, and alternate fine aggregates [61, 62], there have been a few studies conducted on the efficacy of the development of SCC [63] utilising sea sand [64, 65] as an alternate fine aggregate. Therefore, a systematic review [66] was chosen with the goal of offering an in-depth overview on the production of SCC that includes the incorporation of sea sand. Generally, sustainability starts from the construction site itself. Utilizing sea sand [67] in concrete, will help the coastal areas to reduce transportation costs and thus results in sustainability. The study focuses on replacing conventional fine aggregates with sea sand [68] in SCC to help environmental sustainability, improve durability, and decrease construction costs. In this context, availability of marine resources [69, 70] can be utilized.

The rest of the manuscript is organised in the following manner. Literature background is provided in Sect. 2. Section. 3 describes the methodology. In Sect. 4, the advantages of substituting sea sand for the traditional fine aggregate in the

Table 4 Assessment of the physical characteristics of non-treated sea sand (NSS) and desalted sea sand (DSS) obtained from Karatsu harbour of Saga Prefecture, Japan [20]

Sand type	Residue on each sieve size (%)							Physical properties				
	5 mm	2.5 mm	1.2 mm	0.6 mm	0.3 mm	0.15 mm	< 0.15 mm	Fineness modulus	Density (g/cm^3)	Water absorption (%)	Chloride (%)	Sulphate (%)
NSS	0.0	6.2	23.7	30.3	27.9	10.6	1.3	2.83	2.60	1.33	0.1968	0.0860
DSS	0.3	8.3	21.8	28.7	32.8	7.1	1.0	2.89	2.60	1.31	0.0054	0.0090

Table 5 Permissible limits of the properties of the sea sand [15, 34]

Properties	Permissible limits (%)
Sediment content	< 1.0
Sea shell content	< 3.0
Cl^-	< 0.03
SO_3/SO_4^{2-}	< 1.0
Ruggedness	< 8.0

Table 6 Physical properties of the standard sand [35]

Particle size	Percent (%)
Between 1 mm and 2 mm in size	33.33
Below 1 mm but above 500 µm	33.33
Below 500 µm but above 90 µm	33.33

Table 7 Permissible limits of deleterious substances in fine aggregates [36]

Deleterious substances	Maximum % of fine aggregate by mass		
	Uncrushed	Crushed/mixed	Manufactured
Coal and lignite	1	1	1
Clay lumps	1	1	1
Materials passing through a 75 µm IS sieve	3	15-crushed 12-mixed	10
Soft pieces	Nil	Nil	Nil
Shale	1	Nil	1
Sum of % for all deleterious materials (excluding mica)	5	2	2

production of SCC are discussed. Section. 5 presents the most common advanced alternatives for concrete reinforcement in SCC, incorporating the use of sea sand as a fine aggregate. Section 6 Elaborates the necessity to incorporate sea sand as a fine aggregate. Section 7 presents the major challenge involved in the development of SCC using sea sand. Section 8 addresses the limitations. Section 9 explores the identification of sea sand properties using artificial intelligence. Section 10 focuses on continuous monitoring of sea sand concrete properties in real-time using Internet of Things (IoT). Section 11 emphasizes advancing sustainability with Self-Compacting Concrete (SCC) incorporating sea sand. Section 12 delves into future perspectives, and the conclusions are drafted in Sect. 13.

2 Background

The investigation conducted by Tjaronge et al. [63] have explored the impact of sea sand as well as seawater in manufacturing of SCC. The study demonstrated a satisfactory compression strength of approximately 42.5 MPa on the 28th day [63, 71]. The study acknowledged that the development of Calcium-Silicate-Hydrate (C–S–H) was unaffected by the decreased production of Calcium Hydroxide ($Ca(OH_2)$ / CH) owing to the elevated production of ettringite and Fridel's salt from the 1st day to the 28th day. The researchers performed an empirical study on the concrete performance characteristics, considering the inclusion of sea sand and seawater using two distinct water to binder ratios, namely 0.38 (identified as group A) and 0.28 (identified as group B) [12]. Reference concrete was made by mixing river sand and fresh water (identified as No. 0). Sea sand concrete was made by mixing sea sand and fresh water (identified as No. 1). Also, seawater and sea sand concrete was made by mixing with seawater and sea sand (identified as No. 2). OPC (Ordinary Portland Cement), Silica Fume (SF), and Fly Ash (FA) served as the binding materials for the study. Comparatively to the reference concrete, the compressive strength of the concrete mixes containing seawater and sea sand at the previously mentioned

water ratios was higher. The investigation also highlights the speed up of the hydration reaction due to the presence of the extremely soluble salts found in seawater and sea sand [12, 72]. There was just a 8% variation in compressive strength between sea sand and seawater concrete, sea sand concrete, and ordinary concrete, indicating that the compressive strength is not significantly affected by using seawater and sea sand rather than freshwater and river sand [12].

Sakthieswaran et al. [73] assessed the influence of sea sand on polymer concrete manufactured with epoxy resin. From the study, it was revealed that replacing 15% conventional river sand with marine sand exhibited increased durability and strength in air cured polymer concrete. Additionally, Scanning Electron Microscopy (SEM) analysis demonstrated that the filling ability of sea sand led to fewer voids within the polymer concrete. Moreover, the study is limited to unreinforced concrete applications. Also, Brahim Safi et al. [74] conducted an investigation where they used sea-shells as a substitute for river sand in the self-compacting mortar. According to the investigation, $CaCO_3$ is the major component of sea-shells. The chemical constituents of the sea-shells was in line with the limestone. The CaO component of the sea-shells was higher than the limestone filler. The study reported a reduction in the ease of flow for the SCC mortar from around 240 to 210 mm as the percentage of sand replaced by crushed seashell particles increased from 0% to 100% [74, 75]. The bulk density and porosity increased when substituting less than 50% of the sea-shells, while a slight lessening of the compressive strength happened due to the angular shape of the sea-shells. Additionally, it is evident from the results that the seawater [76, 77] is a viable option for mixing in the manufacturing of SCC. Approximately 70% of the total land area is coastal. It is crucial to explore and utilize coastal resources efficiently [78, 79]. Thus, land resources can be preserved.

While numerous surveys and reviews have explored the utilization of sea sand in concrete production, a systematic literature review that specifically addresses the potential benefits, emerging trends, and challenges associated with the incorporation of sea sand into Self-Compacting Concrete (SCC) with non-corrosive reinforcements, such as FRP, textile reinforcements, AMMCs, coupled with Internet of Things (IoT) and artificial intelligence methods like PointRend and neural networks, along with bibliographic analysis using VOSviewer, has not been conducted to the best of our knowledge.

3 Methodology employed

A Systematic Literature Review, or SLR, consists of systematic data collection, critical analysis, synthesis, and presentation of data from various research papers regarding a specific topic [80, 81]. The SLR procedure permitted a thorough comparison of numerous approaches and theories in the pertinent field, assisting in choosing the most appropriate methods and theories for further research. Accordingly, the aforementioned SLR provides a wider and more precise comprehension compared to a conventional literature review, following PRISMA guidelines [66].

The purpose of the SLR is to acquire knowledge regarding the advantages of using sea sand in the production of SCC, to comprehend the acceptable limits of sea sand properties, to grasp the various approaches to enhance the effectiveness of sea sand, and to explore the most prevalent alternatives for concrete reinforcement that incorporate sea sand. The study aims to make a valuable contribution to research by thoroughly examining the use of sea sand [82] in SCC. The decision to adopt the SLR methodology [83] was motivated by the realization of its numerous advantages in achieving the goals of the research.

3.1 Research questions

Formulation of Research Questions (RQs) is a crucial step in extracting and analysing the inherent knowledge of the domain. Four research questions were developed to effectively address the main purpose of the investigation, as outlined below.

RQ1: What are the permissible limits for the characteristics of sea sand to employ it as a fine aggregate in the manufacturing of SCC?

RQ2: What is the impact of sea sand on the workability, setting time, hydration products, strength, and durability of SCC?

RQ3: What are the different approaches to enhance the effectiveness of sea sand in the production of SCC?

RQ4: What are the most common advanced alternatives for concrete reinforcement in SCC that include sea sand as a fine aggregate?

RQ4: What role do real-time monitoring with IoT and artificial intelligence methods like PointRend and neural networks play in assessing the properties of SCC utilizing sea sand?

Table 8 Keywords employed in the search process

Repository	Search within	Keywords	Search date	Outcomes	Requirements
Scopus	All fields	"Sea Sand" AND "Self compacting concrete"	22nd, June 2023	526	Limit to English limit to article
Web of science	All fields	"Sea Sand" AND "Self compacting concrete"	22nd, June 2023	7	Limit to English
Scopus (grey)	All fields	"Sea Sand" AND "Self compacting concrete"	22nd, June 2023	30	Exclude article exclude review
Total				563	

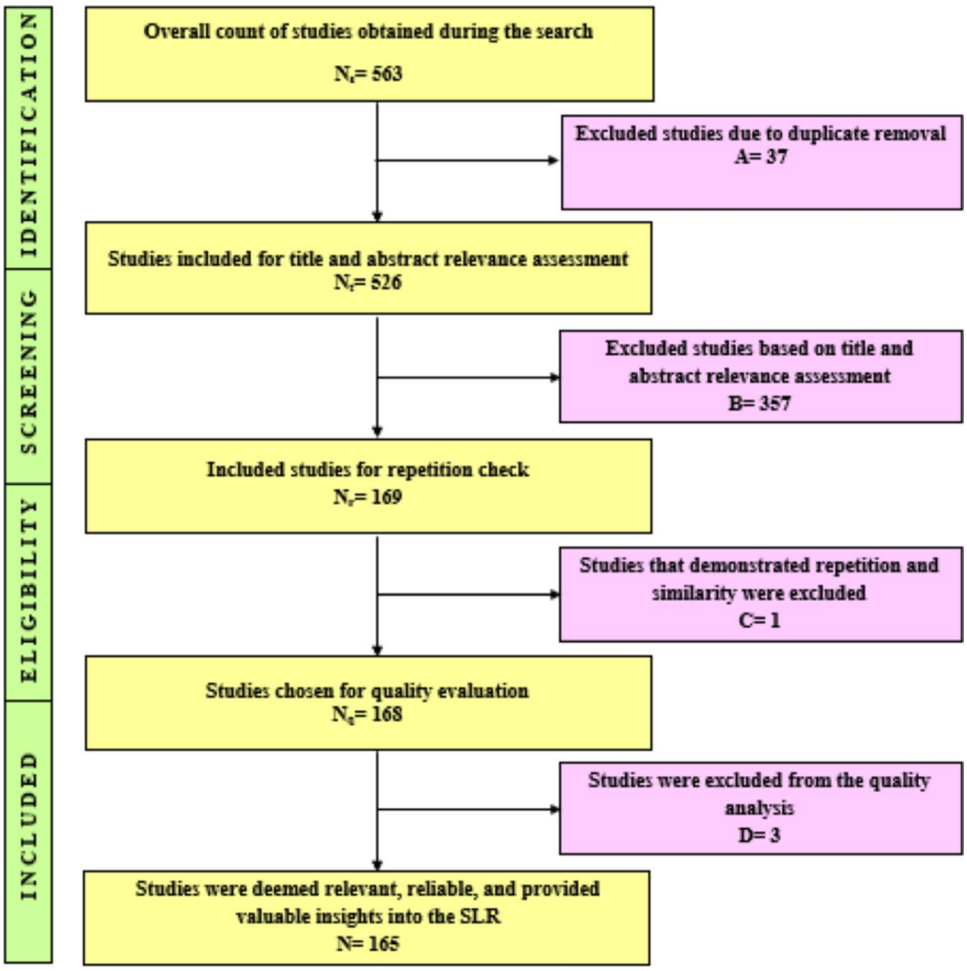

Fig. 6 Systematic Literature Review (SLR) approach recapitulation

3.2 Search strategy

The outline of the SLR process is depicted in Fig. 6. The relevant articles were collected from Scopus and the Web of Science databases. The specific phrases or keywords used in the search process are documented in Table 8.The papers were initially selected by carefully evaluating their title, keywords, and abstracts. The recapitulation of the SLR involves a thorough analysis of the selection of relevant studies from a pool of 563 studies. In Scopus, 526 studies were found, excluding grey literature. Additionally, 30 grey literature sources were separately discovered in Scopus. There were 7 articles found in Web of Science, all of which were articles. In total, 563 studies were retrieved from both Scopus and Web of Science. After eliminating 37 duplicate studies, 526 studies were selected for abstract and relevance screening. During this process, 357 studies were excluded based on the relevance of their abstracts and titles. Subsequently, 169 studies were included for repetition and similarity checks. Out of the 169, 1 study was excluded due to duplication and similarity. For quality evaluation, a total of 168 studies were selected. Out of these,

3 studies were excluded during the quality analysis. Finally, 165 studies, which were considered potentially relevant, reliable, and provided valuable insights into the SLR, were chosen.

Grey literature is an important resource in research, providing valuable insights, diverse perspectives, and up-to-date information that is not found in conventionally published articles. In the Scopus search, all the results excluding journal articles were categorized as grey literature due to their inconsistent levels of quality and credibility. The features and functionalities offered by Microsoft Excel were used to compile the list of articles and execute the steps involved in the SLR. Furthermore, Origin and VOSviewer tools were used to produce visualizations, charts, and graphs for the visual depiction and interpretation of the data. The search outcomes obtained from the databases were documented as lists on the corresponding database platforms. Following that, the lists obtained were imported into Excel worksheets, where a main working sheet was created to combine and arrange all the outcomes.

On the main working sheet, additional screening procedures were conducted, which encompassed examining duplicates, evaluating titles and abstracts, and performing similarity checks.

3.3 Data analysis

Throughout the process of data retrieval, relevant information was gathered from various sources, and the studies were categorized based on standard attributes, such as the publication year and publisher. The database search provided a year-by-year trend of publications until the year 2023, with the count only being available up to the month of June, as shown in Fig. 7.

The contributions made by individual publishers in the context of the topic of interest are as shown in Fig. 8. By analysing the publisher-wise contribution, researchers and readers can gain profound insights into the distribution of content and the influence of different publishers in the field. It highlights the extent to which each publisher has been involved in the publications included in the list. Additionally, VOSviewer [84] was employed to create visual representations of the carefully curated list of works. The resulting network visualization provides a clear and intuitive representation of the connections and collaborations among authors within the research domain. Furthermore, it offered a clear and comprehensive understanding of the notable authors who made significant contributions to the research objective, as shown in Fig. 9. As visualized in the Fig. 10, the primary countries that played a vital role in the incorporation of sea sand in concrete were also included. In 2014, China's demand for sand and gravel stood at 140 million metric tons, projected to increase to 250 million metric tons by 2030 [85]. This necessitates China's increased utilization of sea sand in construction, as depicted in Fig. 10 through bibliographic analysis by VOSviewer.

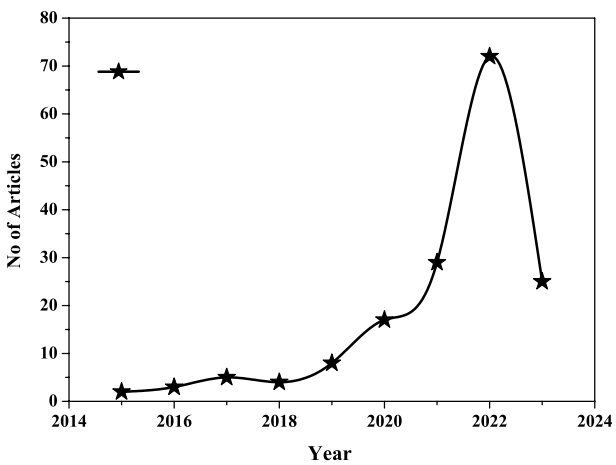

Fig. 7 Obtained year-wise publication trends from Scopus database records

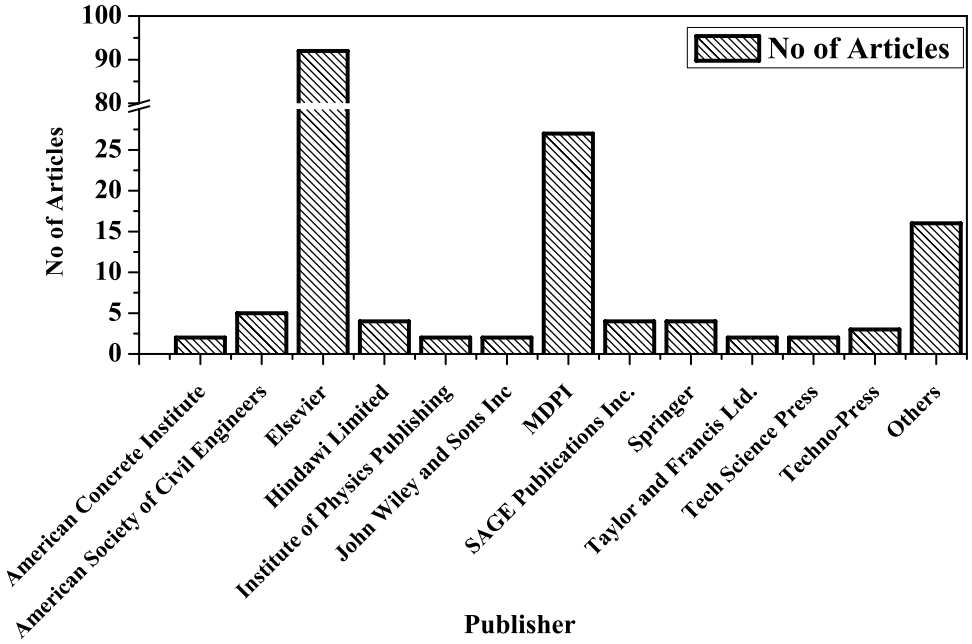

Fig. 8 Contribution of each publisher for the SLR

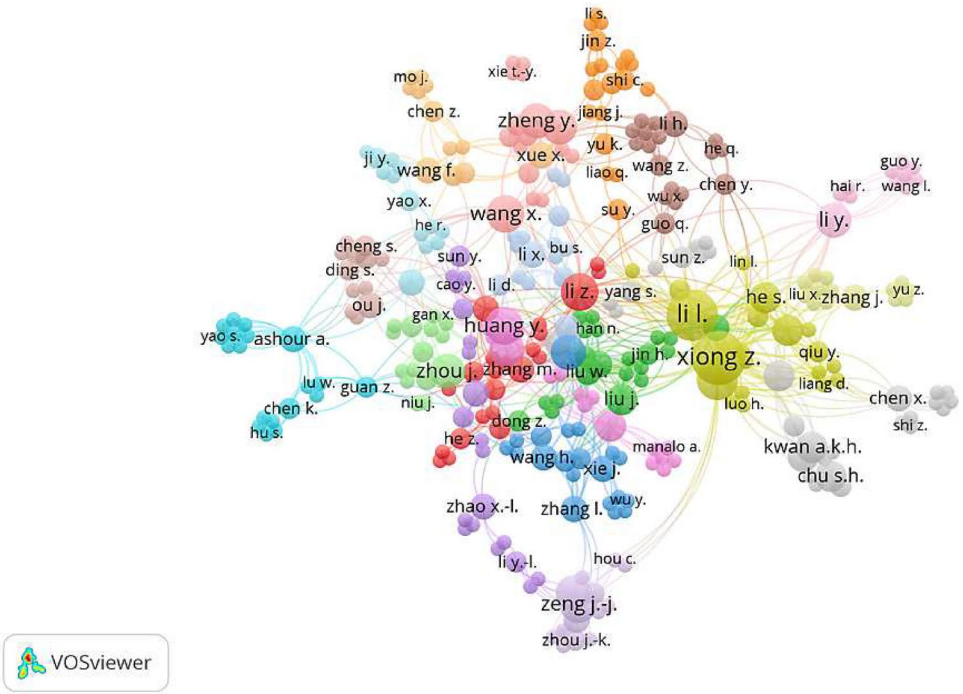

Fig. 9 Network visualization to depict the author-co-citation

4 Advantages of substituting sea sand for the traditional fine aggregate in the production of SCC

4.1 Workability and setting time

In the initial period of 3rd and 7th day, the existence of chloride ions within the sea sand accelerated both the cement setting process and the pozzolanic reactivity of Fly Ash (FA), resulting in an augmentation in compressive strength [20].

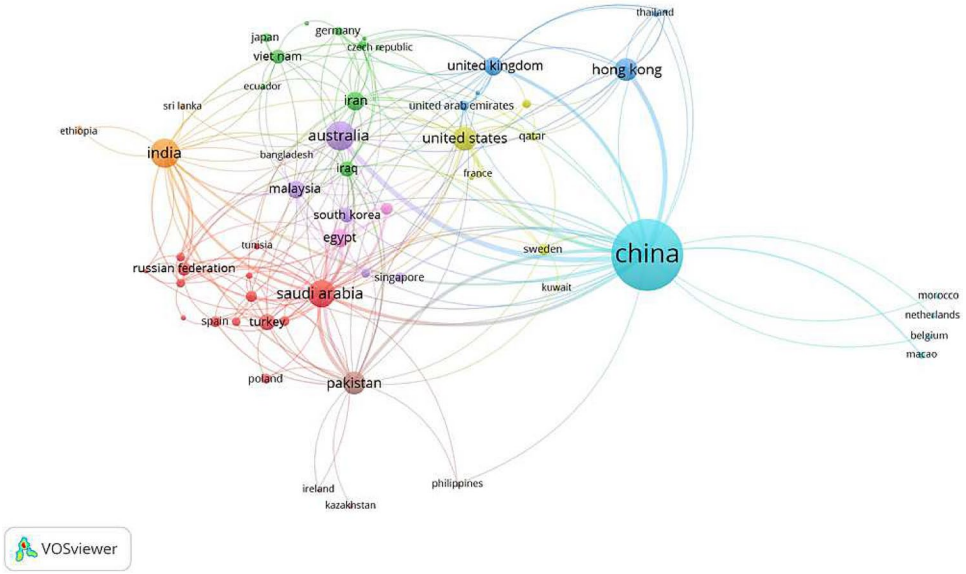

Fig. 10 Network visualization of country-wise citations

A study conducted by Vitalii Kryzhanvskyi et al. [86] demonstrated an increase in the slump flow of SCC when incorporating sea sand, as illustrated in Fig. 11. The study focused on the impact of sea sand on the characteristics of high-strength textile-reinforced SCC. The research revealed that SCC incorporating sea sand exhibited a slump of 620 mm, density of 2305 kg/m^3, and air content of 4.6%. In comparison, the control concrete, using traditional fine aggregate, demonstrated a slump flow of 610 mm, density of 2315 kg/m^3, and air content of 4.8%. Additionally, the study reported that the slump flow was in circular and achieved a slump flow of 680 mm without any segregation. A reach of 500 mm slump was achieved in just 3 s [63].

Aggregate type influences flow characteristics in concrete. River gravel, with its smoother and rounder surface, results in lower viscosity and yield stress [87]. In contrast, Unprocessed sea sand led to a reduction in the workability of freshly mixed concrete, as illustrated in Fig. 12. This effect was attributed to a higher content of fine particles, passing through the 0.3 mm sieve, were found in Non-Treated Sea Sand (NSS) compared to Desalted Sea Sand (DSS). This higher fine particle content can raise the water demand in concrete, resulting in reduced fluidity in fresh concrete. Consequently, concrete utilizing NSS exhibited lower initial slumps compared to those using DSS [20]. However, this effect can be mitigated by the addition of fly ash [20, 88].

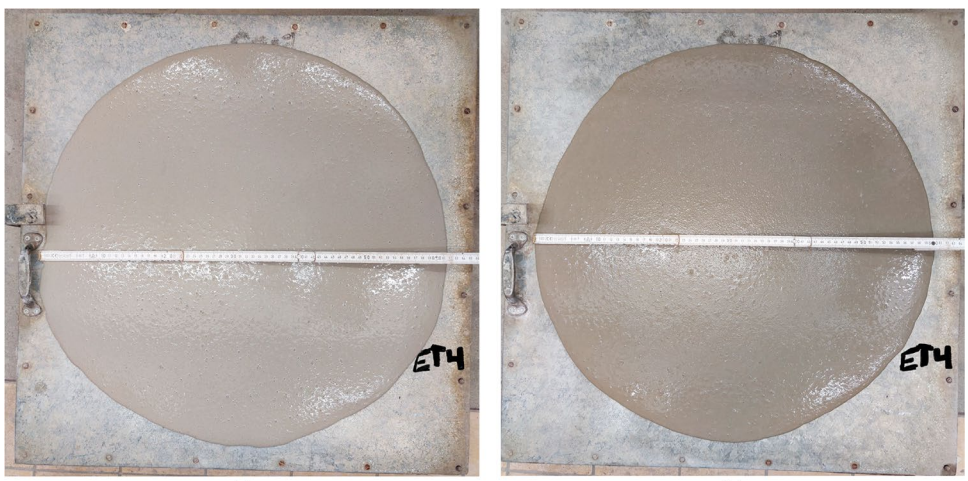

(**a**) (**b**)

Fig. 11 Slump flow of SCC: with sea sand (**a**), control concrete mixture (**b**) [86]

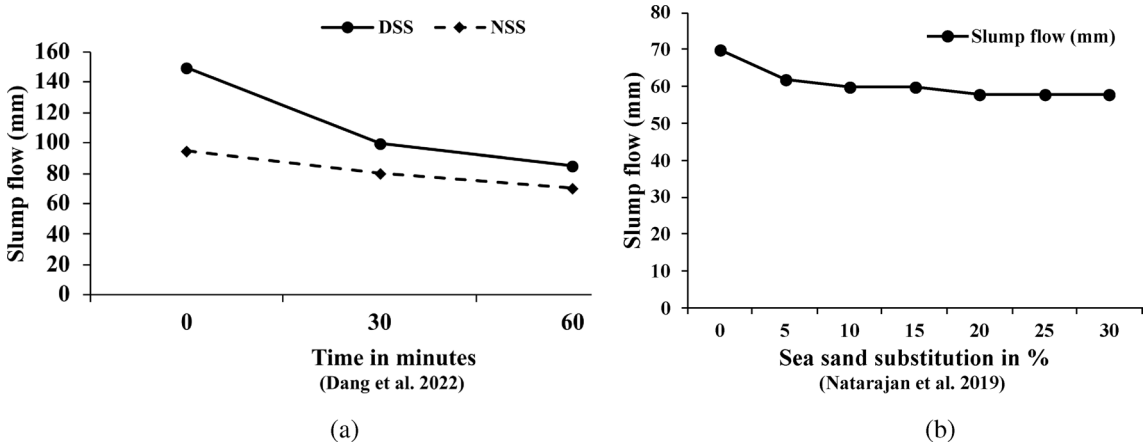

Fig. 12 Reduction in workability due to the addition of NSS [14, 20]

4.2 Hydration products

Chloride ions speed up the cement hydration process [89]. The introduction of seawater in the mix did not exacerbate the chloride permeability because of the Friedel's salt (Fs) formation [90]. The utilization of mineral admixtures reduced permeability. Integration of sea sand, seawater, and Supplementary Cementitious Materials (SCMs) has improved electrical resistivity and increased resistance to chloride penetration in Ultra-High-Performance Concrete (UHPC) mixes prepared based on SWSS-UHPC. This was due to the disconnected pore structure resulted from the production of Friedel's salt [91]. The chloride ions within Non-desalted Sea Sand (NSS) can react with tricalcium aluminate (C_3A) and calcium hydroxide (CH), leading to the formation of Friedel's salt ($3CaO \cdot Al_2O_3 \cdot CaCl_2 \cdot 10H_2O$). Conversely, Aluminum Oxide (Al_2O_3) present in Fly Ash (FA) and Blast Furnace Slag (BFS) can promote the generation of Friedel's salt The process of Friedel's salt formation can be explained using the provided equations 1, 2, 3 [92].

$$Ca(OH)_2 + 2NaCl \rightarrow CaCl_2 + 2NaOH \tag{1}$$

$$3CaO \cdot Al_2O_3 + CaCl_2 + 10H_2O \rightarrow 3CaO \cdot Al_2O_3 \cdot CaCl_2 \cdot 10H_2O \tag{2}$$

$$3Ca(OH)_2 + CaCl_2 + Al_2O_3 + 7H_2O \rightarrow 3CaO \cdot Al_2O_3 \cdot CaCl_2 \cdot 10H_2O \tag{3}$$

4.3 Strength

Pan et al. [12] found that concrete made from sea sand demonstrated superior compressive strengths at 3rd, 7th, and 28th days when compared to standard concrete. Regardless of exposure conditions and the replacement of supplementary cementitious materials (SCMs), the compressive strengths of NSS concretes consistently exceeded those of DSS concretes at the same age [92]. A similar effect by the NSS concrete can be observed in the Fig. 13. The 7th day compressive strength of Recycled Aggregate Sea Sand Concrete (RASSC) ranged from 42.8 to 47.8 MPa, surpassing the specified design strength. The strain values of concrete produced using seawater, marine sand, Portland Composite Cement (PCC), and crushed river sand closely resembled to those of conventional concrete produced with Ordinary Portland Cement (OPC) and freshwater [93]. The tensile strengths of Sea Sand Concrete (SSC) were found to be higher compared to those of Ordinary Concrete (OC) [94]. The empirical study, which focuses on the manufacturing of M30 coral concrete, acknowledges that the consumption of ocean resources speeds up offshore construction [95]. The research reveals that higher applied loads considerably contribute to coral concrete damage, as escalating internal cracks lead to worsening deterioration and a steady drop in observed ultrasonic velocity [96]. With 40% Recycled Concrete Aggregate (RCA) replacement to coarse aggregate, adding 3% SF and 20% FA to Recycled Aggregate-Seawater-Sea sand Concrete (RASSC) achieved a remarkable 47.7 MPa compressive strength, highlighting the efficacy of the dual mineral admixture for enhancing concrete strength [97]. Analyzing the three-dimensional air void arrangement shows that incorporating fine aggregate with varying particle sizes improves the characteristics

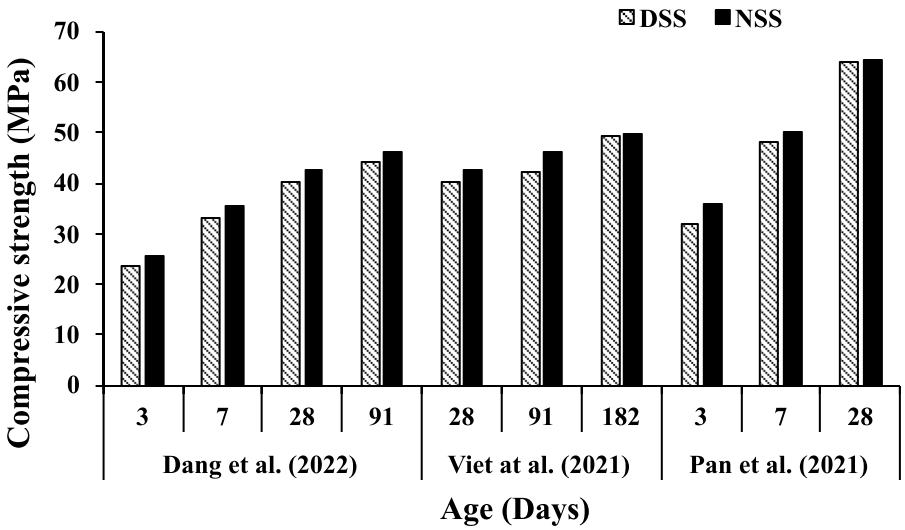

Fig. 13 Compression strengths of DSS and NSS concrete [12, 20, 92]

of the air void system. In each group of high strength fiber reinforced mortar, the number of air voids decreased from 12,446 to 6,652 with an increase in the specific surface area of the fine aggregate. Additionally, Using desert sand as the fine aggregate decreased air void content in the fiber-reinforced mortar from 1.21 to 0.98%, significantly improving air void structure characteristics. Prudent usage of desert sand holds promise for significantly improving both the pore structure and compressive strength. However, similar to desert sand, sea sand is also finer in nature, so the same effect can be seen when sea sand is used [98]. Furthermore, the mix design was conducted as per IS 10262–2019, and the specimens cast as per IS standards [32, 36] demonstrated that the sea sand replaced with fine aggregate up to 100% has led to the enhanced split tensile strength [99], and compressive strength in the developed concrete due to the pore refinement by finer particles of the sea sand [25, 100]. The mechanical properties of concrete produced using untreated sea sand surpassed those of concrete made with desalinated sea sand, irrespective of curing duration, FA or BFS substitution, or carbonation effects [60]. Sea Sand Concrete (SSC) and seawater concrete had a compressive strength of 50.90 MPa, while plain concrete had a compressive strength of 49.34 MPa. This strength parameter shows that the inclusion of sea sand and seawater does not affect the strength [101]. The conclusion from the study demonstrated that adding seawater favored the early-age characteristics of the paste when the water to binder ratio was extremely minimal, resulting in increased compressive strength at an early age [102]. A similar observation was noted in another study, where the presence of chloride ions within the sea sand accelerated both the cement setting process and the pozzolanic reactivity of fly ash (FA), leading to an augmentation in compressive strength [20]. Rough surface texture of sea sand aided in strengthening the connection between material particles and the hydrated gel [18].

4.4 Durability

Concrete durability relies significantly on surface quality, impacting fluid or aggressive substance penetration [92]. The study revealed that the chloride ions, introduced through Dredged Marine Sand (DMS), resulted in a 20–50% reduction in the carbonation of DMS concretes. Improved resistance to carbonation helps to diminish the possibility of deterioration of the steel reinforcement [11]. Furthermore, the samples were subjected to various designated temperatures, varying from 100 to 1000° C. The most significant decrease in mass occurred when the temperatures were below 200° C, and the most significant mass loss corresponded to the moisture content existing in the combinations. The presence of sea sand, and seawater had no impact on the declining mass pattern [10]. The inclusion of superplasticizers and rust inhibitors, such as a polyurethane coating and a zinc-rich epoxy primer [103], contributes to enhancing the performance of Self-Compacting Concrete (SCC) incorporating sea sand [45, 104]. In the study [105], it was observed that subjecting Sea Water Sea-Sand Concrete (SSC) to thermal cycling at 60° C does not degrade its microstructure. The utilization of sea sand in SCC promotes sustainability and durability [106–108]. Increased formation of crystalline hydration products reduced the permeability to chloride ions, autogenous shrinkage, in Sea-Water Sea Sand (SWSS) Concrete [89].

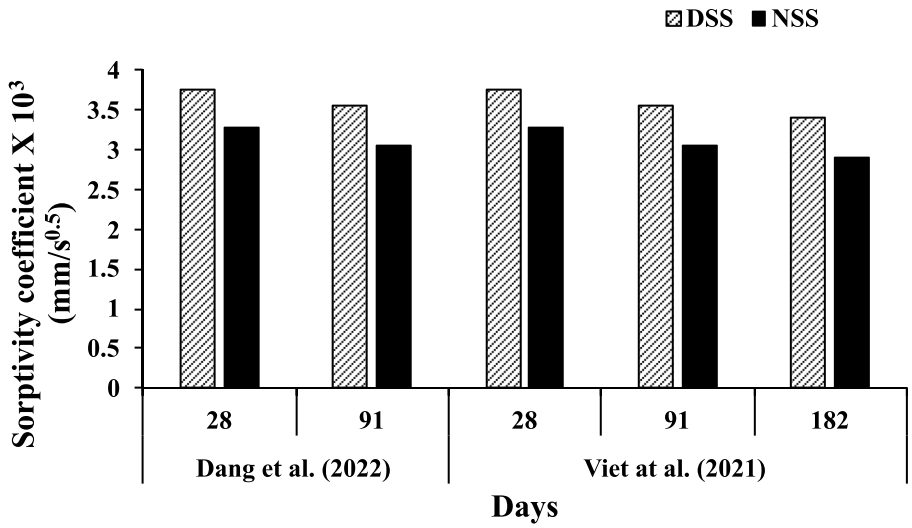

Fig. 14 Sorptivity of NSS and DSS concrete [20, 92]

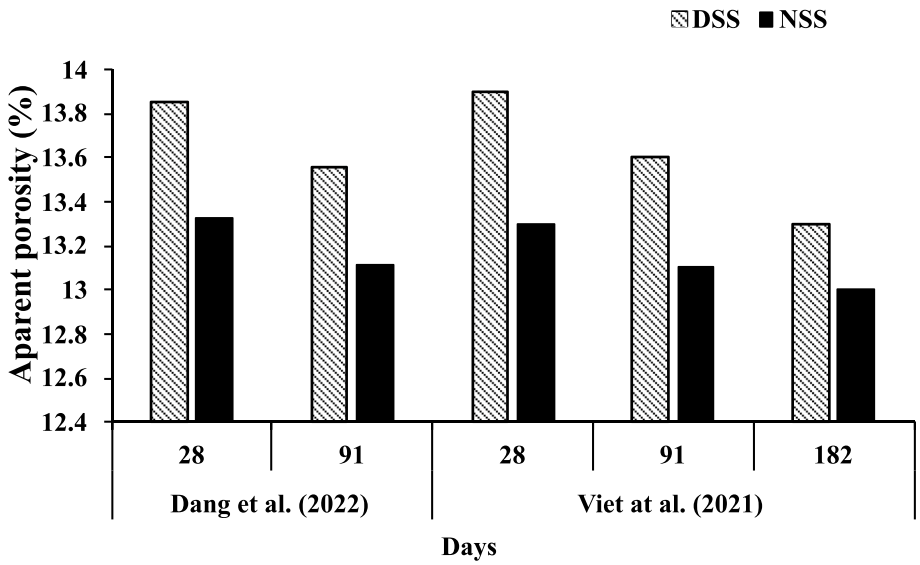

Fig. 15 Aparent porosity of DSS and NSS concrete [20, 92]

4.4.1 Sorptivity

The sorptivity test evaluates a material's capillary absorption and transmission of fluids, serving as a chemical durability measure as it reflects the resistance to external aggressive agents [92, 109]. Sorptivity of NSS and DSS concrete is as illustrated in Fig. 14. NSS concretes consistently demonstrated lower apparent porosity when compared to DSS concretes at both 91 and 182 days [20, 92]. This is attributed to chloride ions interacting with cement hydrate products, forming Friedel's salt and refining the microstructures of NSS concrete compared to DSS concrete [92].

4.4.2 Aparent porosity

Despite variations in SCMs and exposure conditions, NSS concretes consistently demonstrated lower apparent porosity when compared to DSS concretes at both 91 and 182 days [20, 92] as illustrated in Fig. 15. The porosity reduction is evident due to the chloride ions from sea sand, in conjunction with FA or BFS (Blast Furnace Slag), in comparison to ordinary concrete at 91 days [20]. This was attributed to the densification of the matrix by the formation of Friedel's salt [102].

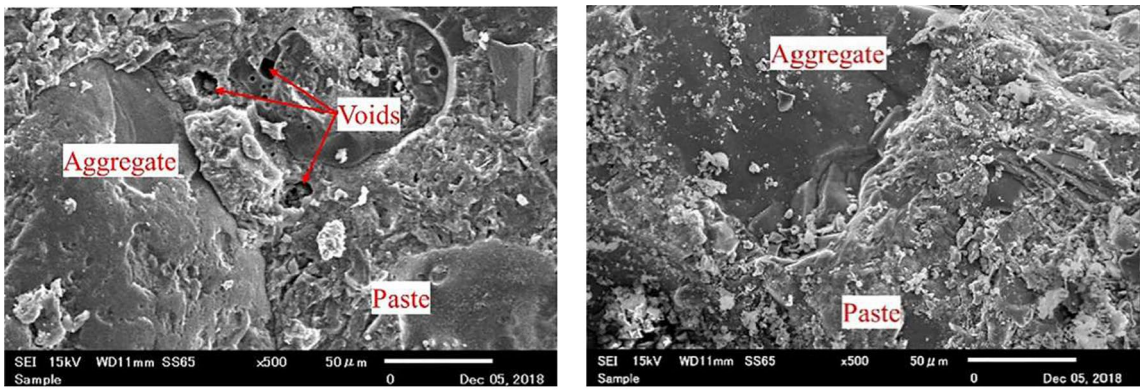

(a) DSS (b) NSS

Fig. 16 Scanning electron microscope (SEM) images of DSS and NSS concrete [92]

Table 9 Quantity of the ingredients used in the M2 and M3 mixes [112]

Mix designation	Mix proportions
M2	Cement—300 kg/m^3, Fly ash—0 kg/m^3, GGBS—250 kg/m^3 (25%), water—155 kg/m^3, Saline Sand (F.A)—700 kg/m^3, C.A.—1050 kg/m^3, water to biner ratio 0.28, Superplasticizer 5 kg/m^3
M3	Cement—245 kg/m^3, Fly ash—200 kg/m^3 (30%), GGBS—105 kg/m^3 (25%), water—155 kg/m^3, Saline Sand (F.A)—683 kg/m^3, C.A.—1072 kg/m^3, water to biner ratio 0.28, Superplasticizer 4 kg/m^3

4.4.3 Microstructural studies

The findings obtained through SEM analysis acknowledged the densely compacted micro-structure in the seawater-based paste at its initial hydration stages, in contrast to its fresh-water based counterpart. Nonetheless, as time progressed, the micro-structures started to resemble one another [110]. According to several research findings, salt possesses limited permeability and porosity, primarily due to the lack of significant open voids within the substance [111]. Additionally, Fig. 16 illustrates Scanning Electron Microscope (SEM) images of non carbonated DSS and NSS specimens. The microstructure of non-carbonated OPC-DSS in Fig. 16a, appeared more porous compared to that of OPC-NSS concrete shown in Fig. 16b. The observations align with the study, where increased formation of crystalline hydration products reduces the permeability to chloride ions and autogenous shrinkage in Sea-Water Sea Sand (SWSS) Concrete [89].

Sang et al. [112] studied the durability of the haro specimens and tetrapod specimens in the real marine environment for 812 days, as shown in Fig. 17a. The M2 mix exhibited the greatest strength result, while the M3 mix showed the least strength results. Hence, these mixes were chosen for further evaluation of their durability. Furthermore, the compressive strength values for specimens M2 and M3 were as follows: their 28th day strengths were 72.2 and 51.0 MPa respectively, before being exposed to sea conditions. After 812 days in the sea environment, their strengths were then determined to be 73.0 and 49.0 MPa respectively. Notably, regardless of the concrete mix employed, the disparity in compressive strength before and after being exposed to the marine environment was minimal, remaining below 5%. This implies that the decline in compressive strength brought on by marine conditions can be effectively countered by adding GGBS or FA to the concrete mix incorporating sea sand in the right amounts. The quantity of the ingredients used in the M2 and M3 mixes are as shown in Table 9. Figure 17b, c displays micro-graphs of the SEM-tested samples of hydration products in specimens M2 and M3, magnified 1000 times. The micro-structures of the specimens were remarkably compacted, and the dominant region had no discernible pores. Instead, discrete clusters of flocculent C-S-H were visible and easily distinguished. Additionally, the M3 specimen's composition had micro-cracks.

(a) In the real marine environment, Haro and Tetrapod specimens

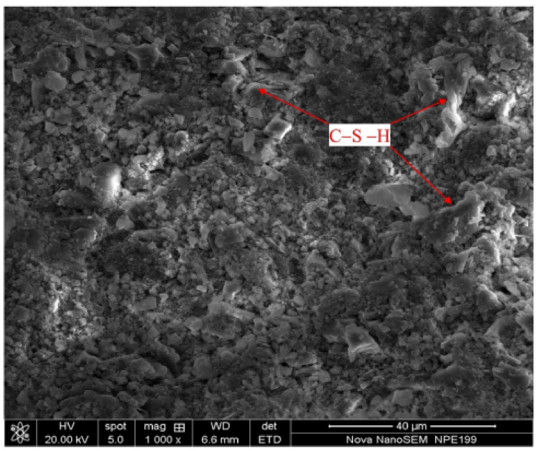

(b) M2 specimen

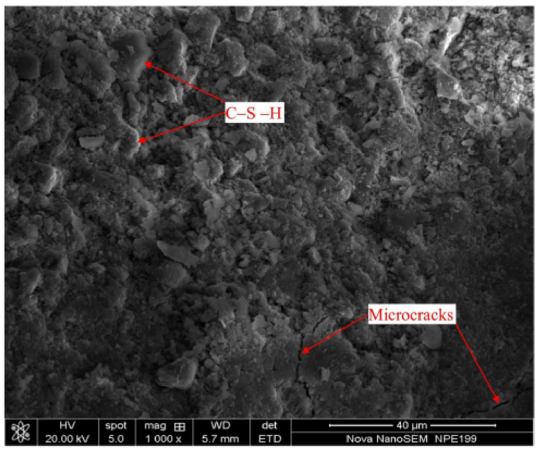

(c) M3 specimen

Fig. 17 Haro, Tetrapod specimens and the morphology of hydration products in specimens M2 and M3 [112]

4.5 Other alternative fine aggregates

Aggregates will fill approximately 75% out of the entire concrete volume. In this context, the quality of aggregates is very important. Aggregate properties can alter the durability and structural performance of the concrete. Generally, the lower limit size of the sand will be about 0.07 mm or a little less. The most common minerals present in aggregates are Iron oxide minerals, Silica minerals, Zeolites, Carbonate minerals, Iron sulfide minerals, Ferromagnesium minerals, Sulphate minerals, and Clay [113]. Studies have been conducted on the necessity of employing alternative fine aggregates in the production of SCC and the utilization of alternate fine aggregates [41, 114]. Large amounts of Marine Dredged Sediment (MDS) are generated annually, posing environmental challenges when disposed of as waste. To address this, MDS can be repurposed for in-situ Marine Sediment Concrete (MSC) production, minimizing disposal and utilizing resources for coastal engineering [115]. However, replacing up to 25% of ultrafine dredged sand resulted in decreased porosity. Also, after 28 days, there was an improved compressive strength of 43.8 MPa [116]. Favourable outcomes in terms of durability were obtained when 50% of river sand was replaced with m-sand [117]. The maximum compressive strength in cement-based materials is achieved by incorporating desert sand in the range of 20–40% [118]. In the M30–M60 concrete strength range, substituting 20% desert sand produced modestly favourable benefits, while up to 60% replacement remained acceptable. However, excessive substitution could harm the characteristics of concrete. For M80 strength concrete, desert sand replacement mostly had negative effects, with

a 60% limit proposed. Finally, the employing of desert sand is discouraged for M100 concrete [119]. The researchers discovered improved flowability and reduced rheological properties like plastic viscosity, and yield stress when river sand was employed as a replacement for micro silica as a fine aggregate. This trend was more noticeable with larger river sand particles [41]. The study of concrete grades M30 and M65, developed using manufactured sand at curing times of 7, 28, 56, and 91 days revealed approximately identical strength values to those observed in ordinary concrete [61]. The test results revealed that concrete containing 30% Treated Used Foundry Sand (TUFS) showed greater impermeability and durability characteristics than control concrete [62]. Using recycled aggregate from construction and demolition waste reduces the need for natural aggregate in new concrete, promoting sustainability [120, 121]. While, the addition of Silica Fume (SF) and Fly Ash (FA) enhanced the compressive strength of Recycled Aggregate-Seawater-Sea Sand Concrete (RASSC) by improving interfacial bonding, filling pores in Recycled Coarse Aggregate (RCA), and forming C-S-H gel through a reaction with calcium hydroxide [97]. Additionally, manufactured sand has been used as an alternative to river sand to meet national demand [5]. Replacing river sand with Fine-dune Sand (FS) lowered workability and fresh Unit Weight (UW) in concrete mixes. However, substituting 35% of the cement with GGBFS improved workability and UW in fresh concrete mixes [122].

4.5.1 Particle packing of SCC with sea sand and various other fine aggregates

Previous research indicates that finer sand improves paste performance by reducing yield stress and viscosity, while coarser sand requires higher levels of yield stress and viscosity for satisfactory flowability in the mixture [123]. Additionally, according to Benabed et al. [124], mortars using binary and ternary sand combinations exhibited a significant increase in compressive strength and met the criteria for Self-Compacting Mortars (SCM) regarding slump flow and V-funnel time. However, SCM mixes with higher dune sand content (up to 50%) showed smaller flow diameters and longer flow times compared to those without dune sand or with only 25% dune sand. This is attributed to the fine texture of dune sand, which requires more water and cement than crushed or river sand for optimal fluidity. The same effect was observed in Non-Treated Sea Sand, as reported in studies [14, 20]. The Particle-Size Distribution (PSD) significantly affects the packing density of the granular structure, which in turn determines the volume of voids to be filled with cement paste. Similarly, optimizing the particle-size distribution and packing within a cement-SCM-filler system can lead to the development of more sustainable concrete and improved rheological properties and workability characteristics [125].

4.6 Incorporation of mineral admixtures to improve the performance of SCC utilizing sea sand

The corrosion resistance of the steel bar was significantly improved by blast furnace slag powder with a concentration of over 20% [126]. This finding aligns with the study indicating that fine-grained concrete, with 30–50% GGBFS replacement, is categorized as low chloride penetration concrete, meeting conventional standards for durability and mechanical properties [127]. Limestone-Calcined Clay Cement (LC_3) improved the durability and chemical reaction ability of the concrete. The best shrinkage performance can be achieved with 25% FA. It is evident from SEM results that FA/LC_2 (Calcined Clay and Limestone) can optimize Seawater and Sea sand Concrete (SSC) performance by making the microstructure of SSC coarser and more complex over time [88]. The study examined the characteristics of concrete produced using Marine Dredged Sediment (MDS). Findings indicated that the inclusion of recycled aggregate generally has an adverse effect on the strength of Marine Sediment Concrete (MSC). On the contrary, the strength of MSC improves with the incorporation of SCMs [128]. Consequently, studies have demonstrated improved microstructural properties with the addition of SCMs [129–131]. Heating binders and activator solutions before mixing with aggregates improves fly ash-based self-compacting geopolymer concrete, termed as Reformed Geopolymer Concrete (RGC). RGC outperforms Post-casting Heated Geopolymer Concrete (PHGC) and Control Cement Concrete (CCC). Microstructural analysis reveals that RGC has less unreacted fly ash, explaining its superior properties [132]. As per the study [133], triple mix concrete, consisting of 80% OPC, 5% FA, 10% SF, and 5% nanosilica, exhibited superior fracture toughness and reduced brittleness, making it suitable for reinforced concrete structures subjected to dynamic or cyclic loads. Paste strength was improved by SF [134]. Because of the vast surface area of SF and the poor scattering of Basalt Fibre (BF), the flowability of foam concrete diminishes as the amount of SF and BF increases. A 15% addition of SF increased compressive strength by 46%. The incorporation of BF in the range of 0–3% led to a substantial increase of approximately 88% in the flexural strength of the concrete composite. The most efficacious mineral admixture to lessen the loss of compressive strength was metakaolin (MK), whereas SF improved durability [7]. High-volume fly ash SCC exhibited significantly lower chloride ion permeability than normal concretes [135]. Studied the effects of fine Recycled Aggregate (RA) with GGBS and

limestone powder in the production of SCC. Incorporating GGBS led to higher stiffness in SCC, influenced by changes in the cementitious matrix composition. Nevertheless, it is advisable to limit the fine RA proportion to 50% [136]. Addition of FA enhances workability and ductility while reducing heat of hydration and shrinkage. Ground Granulated Blast Furnace Slag (GGBS) and Silica Fume (SF) improve compressive strength. Rice Husk Ash enhances overall mechanical properties. Ground-glass pozzolans boost early strength gain. Solid waste ceramics improve ductility. Iron Ore Tailings enhance strain-hardening behavior. Magnesium Oxide (MgO) enhances ductility and improves CO_2 sequestration. Calcined Clay Cement (LC_3) refines pores. Calcium Sulfoaluminate (CSA) Cement decreases autogenous shrinkage and enhances initial strength. Hollow Glass Microspheres (HGM) reduce density and enhance fresh characteristics [180]. Researchers studied the effects of fine Recycled Aggregate (RA) with GGBS and limestone powder in the production of SCC. Incorporating GGBS led to higher stiffness in SCC, influenced by changes in the cementitious matrix composition. Nevertheless, it is advisable to limit the fine RA proportion to 50% [136]. The concrete mix comprising 35% GGBFS and 15% FA exhibited better outcomes in terms of splitting tensile strength, and compressive strength after 28 days [137]. The study demonstrated the improved mechanical properties of the seawater-concrete incorporating coal bottom ash [138]. Including GGBS and FA led to the generation of additional hydration products and denser structures, and improved the Interfacial Transition Zone (ITZ) [139]. Concrete incorporating GGBFS exhibited improved density, a lesser overall porosity compared to standard concrete, fewer internal micro-structure flaws and cracks, and exhibited a smaller diffusion coefficient for chloride and iodide ions [140]. The use of FA improved the ability to withstand penetration by chloride ions [141]. A concrete mixture containing the greatest amount of GGBS (250 kg/m^3) performed best in compressive strength, splitting tensile strength, and chloride ion resistance. In contrast, the mixture incorporating the lowest content of GGBS (105 kg/m^3) performed poorly. Furthermore, concrete with GGBS and FA preserved its compressive strength in the marine environment, based on the findings acquired from the on-site samples [112]. Irrespective of environmental conditions and replacement with FA or BFS, chloride ions decreased the observable porosity of concrete after 182 days [92]. The inclusion of metakaolin (MK) demonstrated superior resistance to carbonation compared to both the control group and Coral Sand Concrete (CSC) containing FA and BFS [142]. After 28 days, the concrete blend comprising 10 wt% GGBFS and 10 wt% MK, along with seawater, attained a compressive strength surpassing 50 MPa. Inclusion of MK and GGBFS considerably elevated chloride ion penetration endurance of lightweight aggregate concrete, and drying shrinkage [90]. Micro-structural examinations demonstrated that the inclusion of Calcined Layered Double Hydroxide (CLDH) led to an increase in the quantity of the products formed during the hydration process, including C–(A)–S–H, ettringite, and portlandite [143]. Waste Glass Powder (WGP) exhibits pozzolanic activity. The ideal replacement was found to be 30% 75 μm WGP, activated mechanically and chemically, which enhances strength and minimizes expansion [144]. Findings from the research indicated that the involvement of the blend SF, slag with cement changed when seawater was deployed as the mixing water, promoting hydration and autogenous shrinkage, which is a significant consideration in the manufacturing of Ultra High-Performance Concrete [102]. Integrating SCM with particle packing modelling creates a new low CO_2 cement matrix for high-performance lightweight aggregate concrete, cutting carbon emissions by 43% and enhancing mechanical properties [145]. Innovative concrete that included treated recycled aggregates, seawater, sea sand, and 35% or 50% LC_3 replacement displayed nearly equivalent bond behaviour to other types of concrete [146]. Moreover, a reduction in porosity is evident due to the chloride ions from sea sand, in conjunction with FA or BFS (Blast Furnace Slag), in comparison to ordinary concrete at 91 days [20].

5 Alternative reinforcement for SCC with sea sand as fine aggregate

5.1 Fiber reinforcement

Chloride corrosion in Sea-sand Engineered Cementitious Composites (SECCs) impacts different fiber types uniquely. For Polyvinyl Alcohol (PVA) fibers, it enhances ductility by filling pores and micro-cracks with the products of chloride corrosion but weakens chemical bonding. Conversely, chloride corrosion in Polyethylene (PE) fibers leads to radial cracks, notably reducing ductility [147]. Additionally, the inclusion of both Polypropylene (PP) and PVA fibers alters the compression response of Sea-Water Sea-Sand (SWSS) concrete, transitioning it from brittle to ductile failure modes [148]. Furthermore, the combination of glass fiber and expansive agent significantly strengthens fiber-mortar interfaces, leading to improved ultimate displacements under high strain rates [149]. Additionally, FRP bars, lacking strong bonding ribs, may have weaker bonds than steel bars. Adding fibers and an expansive agent to concrete could help create gripping stresses on FRP bars to address this issue [150]. Glass fiber's tensile strength prevents crack propagation in concrete [151, 152]. According to

the study conducted by Osman et al. [153], the addition of 3% basalt fiber increased flexural strength by approximately 88%. Recycled steel fibers from waste tires improve bond strength between BFRP rebars and fiber-reinforced concrete by up to 6.3% in static and 9.7% in fatigue loading [154]. Basalt fiber (BF) strengthens concrete toughness [155]. Concrete mixes containing 1% and 5% PP fibers show significantly better specific creep properties than other tested geopolymer composites cite137. The utilization of steel fibers considerably improved the ability of the concrete for energy absorption and resistance to repeated impacts [156]. Splitting and fracture tests were conducted to understand the impact of EAs and Glass Fibers (GFs) on the splitting strength and fracture behaviour of SWSS Concrete (SWSSC). According to the study, the suitable percentage range for EAs was 3–6%, and this content increased as the amount of GFs increased [157]. The dominant failure mode noticed in the PVA Fiber-Reinforced Recycled Concrete slabs (PRCB), was the yielding of the longitudinal tensile reinforcement, in addition to a minor occurrence of concrete crushing within the compression zone. Furthermore, there was evidence of PVA fibers being pulled out or broken at the site of cracking. On the other hand, the Recycled Concrete Slabs (RCB) clearly showed concrete collapse within the compression zone, and their ductility did not match the ductility of the PRCB. After assessing workability, compressive strength, and dynamic compressive performance, the optimal percentage of Recycled Tire Steel Fiber (RTSF) for concrete was estimated to be 0.75% [158]. The impressive capabilities of double-helix BFRP fibers were reaffirmed through an analysis of pull-out test findings, which evaluated the mechanical characteristics of normal-strength concrete samples reinforced with different types of macro BFRP fibers [159]. The incorporation of PVA fiber was effective in preventing crack formation and significantly enhancing the ductile properties of the slabs [160]. The test outcomes revealed that the predominant mode of failure pattern in Sea Sand Recycled Concrete Filled Circular Steel tubes (SSRCFSs) was similar to that observed in conventional concrete filled steel tubes [161]. Moreover, in different concrete grades (M35, M65, and M85), the addition of steel fibers had a relatively small impact on the increment of the compressive strength, modulus of elasticity, and Poison's ratio, all of which were under 10 %. Across all concrete grades, fibre doses considerably improve the post-cracking responses [162].

5.2 Fiber Reinforced Polymer (FRP) bars

The primary constraint in concrete structures constructed using sea sand and [163] and seawater [164, 165] is the corrosion of steel bars. The lifespan of concrete structures will be threatened by too many active ions like Na^{+}, Cl^{-}, SO_4^{2-}, Ca_2^{+}, and Mg_2^{+} [72, 75]. In this context, Fiber Reinforced Polymer (FRP) bars have gained much importance to overcome corrosion and to reduce the cost. The confinement effect of the FRP jacket was significantly higher than that of the stainless steel tube [50]. The research objective was to forecast the Interfacial Bond Strength (IFB) between the concrete and of Fiber-Reinforced Polymer Laminates (FRPL) by employing a hybrid ensemble machine learning technique employing the findings of a single shear-lap test. The model called the Hybrid Hensemble (HENS) was the most accurate in making predictions [166]. The existing equations provided by the American Concrete Institute (ACI) are more trustworthy than artificial intelligence models for determining the flexural strength of FRP-reinforced concrete beams. However, the newly developed Gradient Boosting Tree model exceeds the present Gene Expression Programming model in terms of precision [167]. Augmenting the thickness of the FRP can prevent dilation of the specimens [168]. As the term implies, hybridization [169] involves the amalgamation of various materials within a single cross-section of an FRP bar to create a pseudo-ductile bar. Different materials employed in the fabrication of hybrid FRP bars have different ultimate tensile strains, which determine the ductile nature of fabricated FRP bars. Additionally, hybridization improves the elasticity of composite bars, and steel has a linear relationship between elasticity and volume [170]. According to ACI 440.1R-15, when the bonded lengths were more than 10 times the bar diameter (10 db), it was expected that there would be an increased stress level within the bar [171]. The Studies in the literature suggests that concrete splitting failure can be avoided by ensuring a concrete cover that is three times the diameter of the reinforcing bar [172]. Depending on the fiber type, manufacturing technique, load type, and chloride ion environment, FRP bars retained strength between 49% and 77% [89]. Deeper spiral ribs can enhance the bonding strength between FRP bars and Coral Aggregate Concrete (CAC) [173]. The University of Wollongong has recently developed an innovative standing support system. This standing support has an exterior tube constructed of FRP composite, and the inside is filled with concrete produced from coal slag. The infill's strength and ductility were improved by using the high strength-to-weight ratio of FRP composite [174]. According to the experimental findings, FRP-Concrete-Steel Solid Columns (FCSSC) exhibited a significantly greater carrying capacity of axial load when compared to the combination of a hollow steel tube and a concrete filled FRP tube [175]. The Pull Out Test (POT) is popular among the scientific community [176, 177]. In contrast to the beam test, setting up the POT in a laboratory is easier, and similar to the beam test, it delivers accurate results and effectively displays the impact of variables on outcomes. As a result, it appears to be the best choice for investigating the bonding between concrete and steel.

Additionally, it is suitable for the confined bar test [178]. A comprehensive database of pull out results from specimens assists in developing predictive models for the bond strength of steel and Glass Fiber Reinforced Polymer (GFRP) bars in both normal and high-strength concrete [179]. Engineered Fiber-Reinforced Concrete (EFRC) increases tensile strength, enhances ductility, and enhances properties related to shrinkage, impact, fatigue, post-cracking resilience, cavitation, toughness, and erosion resistance while increasing the entire serviceability of concrete [180]. The initial stiffness and yield strength of Concrete-Filled Steel Tube (CFST) columns are only marginally improved by FRP rings, but their final strength is greatly increased. The increased initial stiffness and yield strength of CFST columns are advantageous for design. FRP ring rupture failure occurred in CFSTs that were confined within a FRP ring. Compared to PET FRP, the rupture of CFRP rings proved more explosive [181]. The addition of an FRP jacket significantly enhances the elastic stiffness, yield axial load, and ultimate axial load of Elliptical Concrete-Filled Steel Tube (ECFST) columns. These enhancements in axial yield load and elastic stiffness are valuable for the design of ECFST structural components [182].

[A] *GFRP bars* In comparison to specimens reinforced with steel bars, the bond behaviour of those with GFRP and BFRP bar reinforcements were ductile [183]. This aligns with observations from another studies where GFRP beams showed lower bond strength reduction compared to steel beams [53, 184, 185]. Meanwhile, increasing the diameter of GFRP tube concrete columns boosts their load-bearing capacity and stiffness while preserving some degree of ductility [186]. GFRP spiral stirrups and longitudinal reinforcement prevent diagonal cracking, increase shear capacity, and improve ductility in short concrete columns. The load–displacement curve of columns with GFRP spiral stirrups resembles that of those with traditional round steel stirrups, demonstrating the viability of GFRP bars and spiral stirrups in column construction [187]. GFRP bars exhibit enhanced durability when exposed to salt water along with other saline conditions. GFRP bars, when embedded in a concrete mix similar to that used for CFRP, AFRP, and BFRP bars, demonstrated lower bond strength values. Glass fibre is an extremely popular filament that is isotropic in nature. Popular types of glass fibres include E-glass, S-glass, C-glass, and AR-glass. E-GFRP is the most widely used FRP material because it is the most affordable composite. Due to a shortage of production, BFRP is more expensive than E-GFRP. Utilizing GFRP spiral stirrups and longitudinal reinforcement can avert the development of the main diagonal fissure, boost shear strength, and enhance the flexibility of the short column [188–190]. Compared to the identical beam under room temperature conditions, GFRP-hollow beams experienced an 86.34% reduction in ultimate load, a 36.82% decrease in ductility, and a 92.25% decrease in toughness when exposed to a temperature of 400°C. As compared to GFRP-hollow beams, the performance decline for steel-hollow beams was not as noticeable. In comparison to the same beam tested at room temperature, the steel-hollow beams lost 24.78% of their ultimate load, 17.6% of their ductility, and 63.86% of their toughness when exposed to a temperature of 400°C [191]. The concrete that incorporated 1800 g/m^3 of glass fibers showed the highest mechanical property values. This resulted in a 31.5% enhancement in compressive strength, a 29.9% gain in flexural strength, and a substantial 97.6% enhanced split tensile strength relative to the reference sample [192]. By adding both glass fibers (GFs) and EAs, Seawater Sea Sand Concrete (SSSC) demonstrated an improved compressive strength [193].

[B] *CFRP bars* Comparing CFRP bars to other FRP bars, they are greatly resistant to alkaline solutions, and possess excellent tensile strength. Carbon fibres were suggested for materials with a high elastic modulus, while glass and basalt were favoured for materials with a low elastic modulus. Self compacting light weight aggregate concrete specimens confined only with CFRP or steel fibers exhibited sudden failure and reduced ductility. However, combining CFRP and steel fibers improved the failure modes through collaborative bridging and confinement effects, yielding evident damage indications [194–197]. The experiments revealed that nanomaterials increased the bond strengths between glass/carbon FRP bars [198].

[C] *AFRP bars* Despite being expensive, AFRP is not frequently used because of its poor compressive strength [59].

[D] *BFRP bars* The study focused on the utilization of BFRP bars within sea sand concrete for coastal constructions. The investigation discovered that the deterioration of BFRP bars and sea sand concrete under thermal cycles was primarily attributed to the target temperature and number of cycling times [199]. In a study examining concrete beams incorporating Seawater Sea sand Glass aggregate Concrete (SSGC), it was discovered that the mechanical properties of SSGC beams reinforced using BFRP bars were equivalent to those of traditional concrete beams reinforced with FRP bars [200]. Strain decreased by 7% initially over 90 days without load, then by an additional 0.3% over 6 months under load, depending on initial strain levels [201]. The high bending complexity of cracks under fatigue load can be attributed to basalt fiber's excellent toughness and energy absorption [202, 203]. Also, the study conducted on the seawater sea sand concrete reinforced with BFRP bars showed the primary cause of failure was the occurrence of compressive failure due to bending action [204]. The study is an essential step in expanding the

possible applications of recently developed BFRP bars in the field of pre-stressing [205]. The investigation involved a study on the effects of exposing specimens to an acidic environment to enhance the understanding of durability characteristics of high-strength SCC reinforced with BFRP. The specimens were examined, and it was found that the aspect ratio of 600 demonstrated noticeably greater resistance in specimens placed in both alkaline and acidic conditions in comparison to other aspect ratios such as 350 and 530 terms of dimensional stability, mass loss, and compressive strength [206]. Consistent pre-cracking flexural performance was noted across all the investigated beams. The load at which cracking occurred was not significantly influenced by factors such as the reinforcement ratio, bar diameter, or the specific type of reinforcement used. Owing to variations in elastic modulus and tensile strength, the BFRP, GFRP, and steel-reinforced beams followed a progressive decrease in strain, deflection, and fracture width. Despite this pattern, the flexural strength of the BFRP-SWSSC beam was much higher than that of the steel-SWSSC beam, significantly stronger than the flexural capacity of the GFRP-SWSSC beam [207]. Ecological High Ductility Concrete (Eco-HDC), known for its superior tensile strength compared to conventional concrete, is well suited for casting deck link slabs for bridge decks where negative moments exist. The key factors governing the reinforcement ratio for BFRP bars in the bridge deck link slab design include the maximum crack width limit, the stress and strain limits in Eco-HDC, and the properties of the BFRP bars [208].

[E] *PET FRP bars* PET FRPs are manufactured using recycled materials like PET bottles, so the cost is lower compared to other FRPs [60]. However, PET FRPs are environmentally friendly and thus can be used instead of steel in coastal areas [60, 209].

[F] *Steel FRP bars* Employing Steel Fiber-Reinforced Polymer (FRP) Composite Bars (SFCBs) in Reinforced-Concrete (RC) columns, particularly with high reinforcement or a high inner steel area in SFCBs, is advantageous for minimizing deflections, crack widths, and improving bearing capacity during serviceability limits [210]. Among the tested specimens, the FRP-RC column showed the most notable deflection and crack width, whereas the steel RC specimen showed the lowest values. The columns reinforced with SFRP composite bars (SFCB RC) were positioned in the middle, occupying an intermediate position in terms of deformation and crack width [211]. Findings of the research done on the bars placed in plain and Steel Fibre Reinforced Concrete (SFRC) showed typical rebar pull-out and fracturing failures [212]. Steel-GFRP Composite Bars (SGCBs) possess benefits over steel bars because of their impressive load-bearing capacity and outstanding ductile properties [213].

5.3 Other reinforcements

[A] *Bamboo sticks* Researchers studied the concrete mix of sea sand and seawater reinforced with bamboo sticks. Bamboo Stick Reinforced Concrete (BSRC) compressive strength was elevated by 3.24 and 17.33% respectively, when 0.6% of sticks were added when the length to diameter ratio was 20 and 30. The results of the analysis indicated that bamboo sticks measuring 1 mm in diameter and having a length to diameter ratio of 10 were the most optimal choice for reinforcement, exhibiting the highest compressive strength and Modulus of Elasticity (MOE) [164].

[B] *Exterior high-density polyethylene (HDPE) tube* This considerably improves the failure behaviour while preserving the integrity of the system without causing harm to the confining tube, which maintains elastic response under flexural loading [214].

[C] *Aluminium metal matrix composites (AMMCs)* Alaneme et al. [215] conducted an investigation into the corrosion performance of alumina-reinforced Aluminum (6063) Metal Matrix Composites (AMMCs). The materials used in this study include chemically pure alumina particles with a particle size of 28μm. The matrix is composed of Aluminum 6063 alloy. The detailed composition of the Aluminum 6063 alloy is provided in Table 10. The study [216] revealed that the protective films on both the unreinforced alloy and composite surfaces remain stable and corrosion resistant in a 3.5 wt% NaCl environment, indicating their clear suitability for marine applications. Despite aluminium's advantages in terms of weight and corrosion resistance, its use in concrete reinforcement is discouraged due to a high thermal coefficient of 22.5×10^{-6} m/mK, compared to concrete's 14×10^{-6} m/mK and steel's 12×10^{-6} m/mK. To address this, Aluminium Metal Matrix Composites (AMMCs) with coefficient of thermal expansion 16.93×10^{-6}/°C

Table 10 Composition details of aluminum 6063 alloy [215]

Si	Fe	Cu	Mn	Mg	Zn	Cr	Ti	Al
0.45	0.22	0.02	0.03	0.50	0.02	0.03	0.02	Bal

with 5% of Sic in aluminium matrix, $5 \times 10^{-6}/K$ for Al_2O_3 reinforced with various volume fractions of SiC particles, and $13.5 \times 10^{-6}/K$ for Al reinforced with 30% of carbon fiber offers a promising solution with their diverse properties. In AMMCs, an aluminum alloy acts as the matrix, reinforced with materials like SiC, Al_2O_3, forming Aluminium Metal Matrix Composites (AMMCs). These surpassed the specified 600 MPa value for Fe600 bars, demonstrating a remarkable yield stress of 869 MPa and a significant flexibility parameter, elongation percentage, at 40.87%. This underscores its potential as an eco-friendly alternative material for steel bars in RC structures. Despite the higher production cost, AMMCs offer numerous benefits like high strength, lightweight, and superior corrosion resistance, thus benefiting the construction industry in various ways [216].

[D] *Textile reinforcement* Textile-reinforced concrete (TRC) consists of a rectangular arrangement of non-corrosive fiber bundles produced from materials such as carbon, glass, or basalt. Incorporating sea sand into Self-Compacting High-Strength Concrete (SCHSC) along with textile reinforcement has yielded a tensile strength of 3.6 MPa, aligning closely with the 3.3 MPa strength of the control concrete and suggesting a modest upward trajectory. The performance data for textile-reinforced concrete, regardless of whether utilizing sea or control concrete matrices, demonstrates comparable results. Furthermore, the utilization of textile-reinforced concrete facilitates a reduction in the cross sectional thickness of structural elements, as shown in Fig. 18, providing a means to minimize material consumption and mitigate steel reinforcement corrosion induced by exposure to sea sand [86].

6 The necessity to incorporate sea sand as a fine aggregate

River sand was at a low cost in the beginning due to its abundant availability, but some regions of the earth faced a shortage of river sand due to its increased demand [21, 217].

6.1 Scarcity of the river sand

The construction industry consumes approximately 6–10 tonnes of gravel for every tonne of cement utilized. Based on the reported global annual cement production of 4.1 billion tonnes, spanning across 150 countries, aggregate demand for making concrete in the year 2017 can be estimated to range between 28.7 and 32.8 billion tonnes. China leads the globe in cement production, with an estimated 2.4 billion tonnes produced in 2017. India had produced 270 million tonnes of cement in 2017, whereas the United States had 86.3 million tonnes. In the United States, aggregates are used at a rate of 10 tonnes per tonne of cement. Using this proportion, aggregate demand might approach 50 billion tonnes per year by 2030, assuming annual global cement production increases to 4.83 billion tonnes by 2030. Figure 19 illustrates a comparison of the worldwide utilization of cement, sand, and gravel, including China and other countries [5, 6].

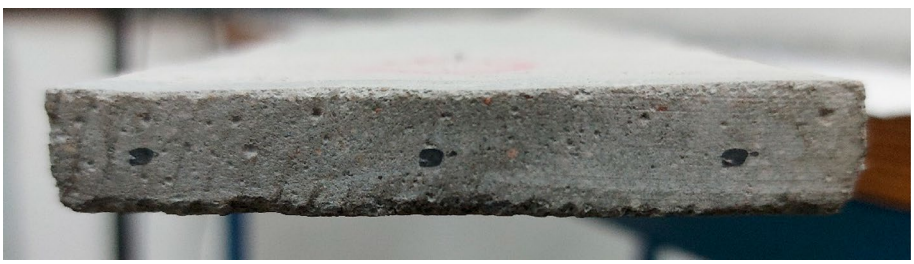

Fig. 18 Cross section of the specimen reinforced with textile material [86]

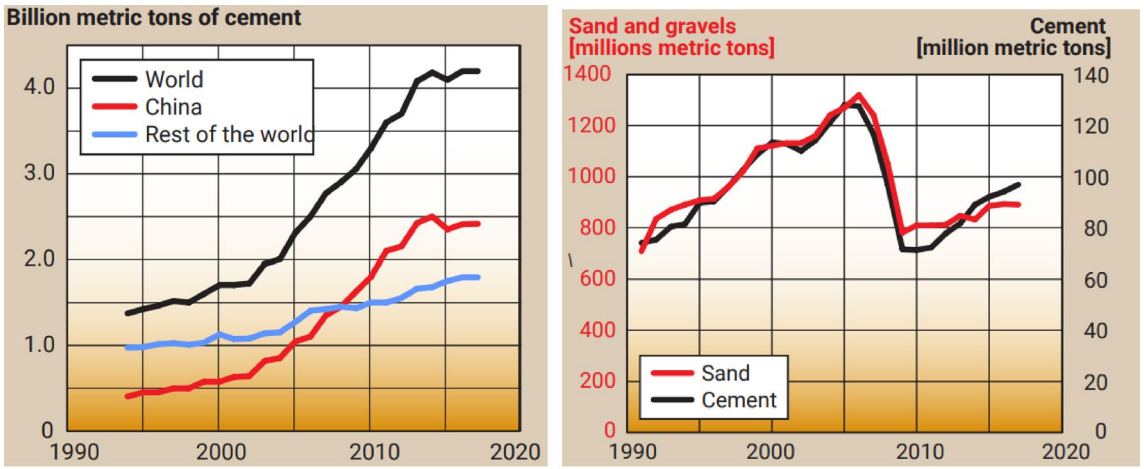

Fig. 19 Global consumption of cement, sand, and gravel among the world, China, and other nations [5, 6]

7 Major challenge in the development of SCC utilizing sea sand

Despite of the advantages, future development of the SCC with sea sand is expected to have the following challenges.

7.1 Corrosion of steel bars

Zhi-Qiang Dong et al. [44] investigated the bond and flexural characteristics of Steel Fiber-reinforced polymer Composite Bars (SFCBS) in concrete incorporating sea sand in simulated seawater for a wet-dry climatic condition for 30, 60, and 90 days. The sand selected was superfine and was sourced from China. Sea sand had a 0.82% chloride ion ratio, which was found out by the chloride ion content test. For the advancement of corrosion, 17.5 g of sodium chloride was combined with 1000 g of mixing water at the time of casting of concrete. The device was prepared at a laboratory in wet-dry cycling conditioned environment to produce the tidal zone of the ocean at the laboratory. To make the artificial seawater, 5% of sodium chloride was added to the tap water. Through the study, they were able to analyse the better performance of steel bar reinforced concrete beams [218] when compared to SFCB RC beams under characteristic loading. Consequently, SFCB reinforced concrete beams performed better in terms of serviceability, which includes crack width, stiffness, and ductility when compared to the steel beam. This being the reason it is a little difficult to say which is better amongst the two types of reinforcement [219]. But SFCBs [44] performed better when compared to steel bars [178] with their mechanisms. Aged steel bar reinforced concrete beams showed increased crack width when compared to aged SFCB beams. The use of sea sand for making SCC is considered as promising research area for the future [24].

8 Limitations

The fundamental objective of the study was to delve into the potential benefits and challenges of incorporating sea sand in the production of SCC. The article collected and assessed the formulated research questions, subsequently constructing a systematic review to explore various research directions and validate the potential of sea sand in the development of SCC. The study comprises a substantial volume of grey literature. However, Google Scholar, the most popular grey literature database, is not included. The keyword "Sea Sand" AND "Self Compacting Concrete" gave 989 results. Also, the keyword Sea Sand AND Self Compacting Concrete gave 25,200 results. The result obtained was oversized. Consequently, despite the meticulous attempts to compile a thorough SLR, some important sources from the grey literature might have been missed. Future scholars who are interested in performing narrative reviews may fill this lacuna.

An additional concern was the time lapse between the commencement of the investigation and the completion of the SLR, during which important advances in the field of research might have taken place. In order to ensure the

SLR was as thorough as possible, manual searching was incorporated to discover the information during the gap time. They were crucial in demonstrating that the research focus had not considerably changed during the interim period. This procedure made it easier to find relevant reviews and pertinent literature in specific research domains, thereby expanding the scope of systematic review and keeping it updated.

9 Identification of sea sand properties using artificial intelligence

Seashells, being fragile, negatively impact the compressive strength of concrete. There were no effective methods for characterizing seashells. In addressing this gap, Tiejun Lieu et al. [13] explored the feasibility of segmenting sea sand photos and analyzing seashells using three common machine learning methods: PointRend, DeepLab v3+, and Trainable Weka Segmentation (TWS). Notably, PointRend exhibited efficient recognition of seashells with diverse shapes, sizes, and surface textures, achieving the highest scores for Intersection over Union (IOU) and pixel accuracy (PA), surpassing followed by DeepLab V3 and TWS as illustrated in Fig. 20.

Hailing Yu et al. [85] explored predicting the strength of sea sand concrete in seawater using artificial neural networks implemented in Python. Evaluating Tanh ANN and Relu ANN models across diverse network configurations, they consistently achieved a mean relative error below 10%. The minimum relative error approached zero, and the maximum relative errors for training outcomes and predictions were 9.79% and 6.85%, respectively. Additionally, the mean relative errors for training and prediction results were 3.82% and 3.16%, respectively. The overall model performance was favourable, with R^2 (Correlation coefficient), MAE (Mean Absolute Error), MSE (Mean Square Error), MAPE (Mean Absolute Percent Error), and E (Efficiency coefficient) values of 0.964, 0.0168, 0.0218, 0.193, and 0.960, respectively. This highlights the model's robust performance, meeting engineering application requirements.

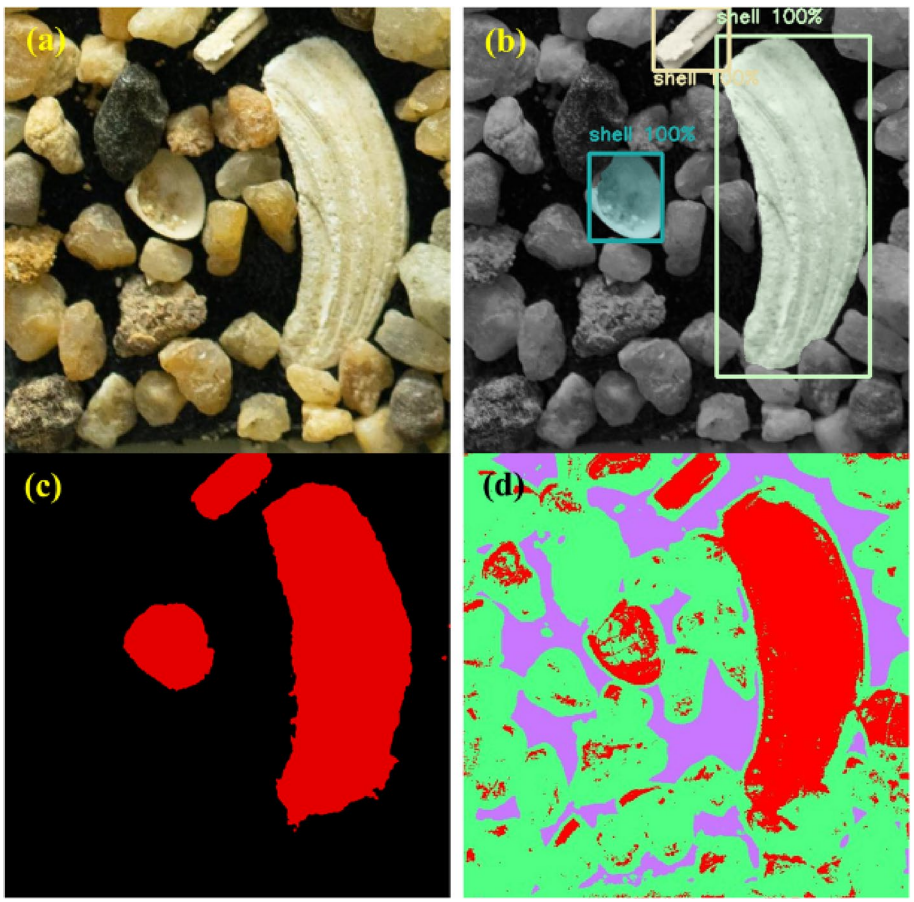

Fig. 20 Comparative Analysis of Segmentation Outputs: **a** Original Image, **b** PointRend, **c** DeepLab V3, and **d** TWS [13]

10 Continuous monitoring of sea sand concrete properties in real-time using Internet of Things (IoT)

The Internet of Things (IoT) is pivotal, utilizing distributed sensors for real-time monitoring and wireless transmission of measurements to a distant user. It's a recommended technology for structural health monitoring. The rise of affordable, continuous monitoring systems based on IoT presents exciting prospects for the future of corrosion assessment in reinforced concrete structures [220]. Over the last decade, sensing devices have been broadly categorized into two main types: potentiometric and fiber optic [221]. Ag/AgCl electrodes are widely utilized [220, 221]. For pH monitoring, typical potentiometric electrodes include Ir/IrO_2, Ag/Ag_2O, Ti/IrO_2, and metallic oxide electrodes. In structural areas, durability monitoring IoT systems can opt for short-range or long-range low-power wireless communication technologies (LPWAN). LPWANs are a preferred choice for IoT applications in monitoring reinforced concrete structures, as they efficiently cover large areas without relay nodes. This choice is also aesthetically preferable due to the reduced number of nodes compared to short-range options. Many of these technologies boast a 10-year battery lifetime, minimizing the need for frequent battery changes during the structure's service life. The implementation of an IoT system in the structure guarantees continuous monitoring and extended data collection.

11 Advancing sustainability with SCC incorporating sea sand

In the anticipated scenario for 2050, there is a fivefold increase in the demand for steel. The production of steel involves substantial energy consumption and results in the release of pollutants, including CO_2 and Particulate Matter (PM) [216]. Choosing traditional steel bar reinforcement may not always be the most efficient solution in terms of density, stiffness, and strength. The increasing importance of non-corrosive reinforcements, such as FRP, textile reinforcements, and AMMCs, is evident as they address these challenges, meeting the growing engineering demands of modern technologies. The PointRend machine learning method is poised to enhance the comprehension of the impact of sea sand on concrete properties, showcasing the accuracy and efficiency of deep learning in analyzing sea sand properties without requiring human involvement [13].

Using an artificial neural network allows for the prediction of the compressive strength of seawater sea sand concrete. The mean relative error for prediction results stood at 3.16%, and the correlation coefficient reached 0.974. This indicates the feasibility of establishing a compressive strength prediction model for seawater sea sand concrete through an artificial neural network. In contrast to the conventional mix design approach, the neural network design method can minimize the need for adjustments in mixing proportions, reducing labor, time, and material waste [85]. By harnessing the Internet of Things (IoT), cost-effective continuous monitoring of structures becomes achievable. Through prolonged data monitoring and intelligent analysis, complex non-linear interactions among factors controlling durability can be comprehended. This heightened understanding significantly improves the reliability of structure assessments, assisting stakeholders in strategic proactive maintenance planning and, as a result, prolonging the service life of the structures [221].

12 Future perspectives

The inclusion of various potential substitutes for river sand and the incorporation of sustainable strategies mentioned in the article provide diversified options for researchers and industry professionals, facilitating the usage of sustainable construction practices.

[A] *Evaluation of the long term durability of non-corrosive reinforcements* Future research should focus on the comprehensive evaluation of the long-term durability of SCC incorporating sea sand as a fine aggregate, especially when reinforced with FRP materials, textile reinforcements, and AMMCs.

[B] *Utilization of IoT* The extensive utilization of IoT, specifically by further investigating the practical application of chloride and pH sensors for real-time monitoring of non-corrosive reinforcements.

[C] *Utilization of artificial intelligence* The PointRend machine learning method shows promise in advancing a better understanding of the impact of sea sand on concrete properties. Additionally, there is potential for artificial neural networks to play a crucial role in predicting the compressive strength of sea sand concrete.

13 Conclusions

The article highlights the potential of sea sand as a viable alternative in advanced concrete applications to meet the rising demand for river sand in construction. It provides various alternatives for sustainable construction practices and emphasizes key areas for future investigation, including assessing the long-term durability of non-corrosive reinforcements, exploring the application of IoT, and employing artificial intelligence to study the properties of SCC incorporating sea sand.

The following concisely outlines the key findings from the systematic literature review with bibliographic analysis:

1. The study revealed China's global leadership in cement production. Additionally, China's demand for sand and gravel is projected to increase 250 million metric tons by 2030, resulting in a greater use of sea sand in concrete production. This trend is vividly illustrated in the country-wise citations network visualization using VOSviewer.
2. In the initial period of 3rd and 7th days, the presence of chloride ions in the sea sand accelerated both the cement setting process and the pozzolanic reactivity of FA, leading to an increase in compressive strength of the concrete.
3. NSS concrete consistently exhibited lower apparent porosity and sorptivity than DSS concretes due to the refinement of the micro-structure through the formation of Friedel's salt.
4. Chloride ions introduced through sea sand have shown a reduction in carbonation by 20%-50%, thereby decreasing the probability of corrosion in steel reinforcement.
5. The PointRend machine learning technique efficiently detected sea shells. This pioneering characterization method in deep learning is positioned to advance the understanding of the properties of SCC with the inclusion of sea sand.
6. Future studies should focus on extended continuous monitoring through IoT to comprehend how non-corrosive reinforcements, including FRP, textile reinforcement, and AMMCs, influence the behaviour of SCC incorporating sea sand.
7. Future research should concentrate on employing diverse pH sensors, chloride sensors, and artificial intelligence to comprehend the characteristics of SCC incorporating sea sand.

Acknowledgements The authors express their sincere gratitude to Dr. Renuka A, Professor, Department of Computer Science and Engineering, MIT, MAHE, Manipal, for her invaluable guidance and support throughout the preparation of this manuscript. We also extend our gratitude to Manipal Academy of Higher Education, Manipal, Karnataka, India, for their invaluable support.

Author contributions Sindhurashmi B. M.—Conceptualization, Methodology, Formal analysis, Investigation, Visualization, Validation. Gopinatha Nayak—Supervision, Methodology, Resources, Validation, Project administration, Review and editing. Adesh N. D.—Methodology, Formal analysis, Investigation, Visualization, Validation, Review and editing. Vidya Rao—Methodology, Formal analysis, Investigation, Visualization, Validation. Sandhya Parasnath Dubey—Methodology, Formal analysis, Investigation, Visualization, Validation.

Funding Authors declare that no funds were received during the preparation of the manuscript.

Declaration

Conflict of interest The authors declare that they have no known competing financial interests or personal relationships that could have appeared to influence the work reported in this paper.

References

1. Makul N. Modern sustainable cement and concrete composites: review of current status, challenges and guidelines. Sustain Mater Technol. 2020. https://doi.org/10.1016/j.susmat.2020.e00155.
2. Anandamurthy AIMRN, Guna V. A review of fibrous reinforcements of concrete. J Reinf Plast Compos. 2017;36:519–52. https://doi.org/10.1177/0731684416685168.
3. Saranya T, Ambily PS, Raj B. Studies on the utilization of alternative fine aggregate in geopolymer concrete. In: National conference on structural engineering and construction management. Springer; 2019. p. 851–859. https://doi.org/10.1007/978-3-030-26365-2_78
4. Kumar Mehta PJMMP. CONCRETE microstructure, properties and materials, 2001
5. Bhatawdekar RM, Singh TN, Tonnizam Mohamad E, Armaghani DJ, Binti Abang Hasbollah DZ. River sand mining vis a vis manufactured sand for sustainability. In Proceedings of the international conference on innovations for sustainable and responsible mining: ISRM 2020-Volume 1. Springer; 2021. p. 143–169
6. Gallagher L, Peduzzi P. Sand and sustainability: finding new solutions for environmental governance of global sand resources. 2019.
7. Choi SI, Park JK, Han TH, Pae J, Moon J, Kim MO. Early-age mechanical properties and microstructures of portland cement mortars containing different admixtures exposed to seawater. Case Studies in Construction Materials. 2022;16: e01041.
8. Mangi SA, Makhija A, Raza MS, Khahro SH, Jhatial AA. A comprehensive review on effects of seawater on engineering properties of concrete. Silicon. 2021. https://doi.org/10.1007/s12633-020-00724-7.
9. Jawahar SP, Raja S, Franco P, Paul J, Shiny DS. The effect of corrosion on durability of mineral free dredged marine sand containing mortar with various additives. J Balkan Tribol Assoc. 2016;22:3919–35.
10. Li Y-L, Zhao X-L, Singh Raman R, Al-Saadi S. Thermal and mechanical properties of alkali-activated slag paste, mortar and concrete utilising seawater and sea sand. Constr Build Mater. 2018;159:704–24.
11. Liu W, Cui H, Dong Z, Xing F, Zhang H, Lo TY. Carbonation of concrete made with dredged marine sand and its effect on chloride binding. Constr Build Mater. 2016;120:1–9.
12. Pan D, Yaseen SA, Chen K, Niu D, Leung CKY, Li Z. Study of the influence of seawater and sea sand on the mechanical and microstructural properties of concrete. J Build Eng. 2021;42: 103006. https://doi.org/10.1016/j.jobe.2021.103006.
13. Liu T, Ju Y, Lyu H, Zhuo Q, Qian H, Li Y. Identification and analysis of seashells in sea sand using computer vision and machine learning. Case Stud Constr Mater. 2023;18: e02121. https://doi.org/10.1016/j.cscm.2023.e02121.
14. Natarajan S, Neelakanda Pillai N, Murugan S. Experimental investigations on the properties of epoxy-resin-bonded cement concrete containing sea sand for use in unreinforced concrete applications. Materials. 2019;12(4):645. https://doi.org/10.3390/ma12040645.
15. Guo M, Hu B, Xing F, Zhou X, Sun M, Sui L, Zhou Y. Characterization of the mechanical properties of eco-friendly concrete made with untreated sea sand and seawater based on statistical analysis. Constr Build Mater. 2020;234: 117339. https://doi.org/10.1016/j.conbuildmat.2019.117339.
16. Feng B, Liu J, Wei J, Zhang Y, Chen Y, Wang L, Chen Y, Sun Z. Research on properties and durability of desalinated sea sand cement modified with fly ash. Case Stud Constr Mater. 2021;15: e00675. https://doi.org/10.1016/j.cscm.2021.e00675.
17. Karthikeyan M, Nagarajan V. Feasibility study on utilization of marine sand in concrete for sustainable development, 2016. Available: http://nopr.niscpr.res.in/handle/123456789/35058
18. Wang Y, Zhang C, Wang J, Xu Y, Jin F, Wang Y, Yan Q, Liu T, Gan X, Xiong Z. Experimental study on foci development in mortar using seawater and sand. Materials. 2019;12(11):1799. https://doi.org/10.3390/ma12111799.
19. Wang Q, Zhu H, Tong Y, Su W, Zhang P. Bond-slip behaviour of the cfrp ribbed bars anchored with the innovative additional ribs in concrete. Compos Struct. 2021;262: 113595. https://doi.org/10.1016/j.compstruct.2021.113595.
20. Dang VQ, Ogawa Y, Bui PT, Kawai K. Effects of chloride ion in sea sand on properties of fresh and hardened concrete incorporating supplementary cementitious materials. J Sustain Cement Based Mater. 2022;11(6):439–51. https://doi.org/10.1080/21650373.2021.1992683.
21. Thunga K, Das V. An experimental investigation on concrete with replacement of treated sea sand as fine aggregate. Mater Today Proc. 2020. https://doi.org/10.1016/j.matpr.2020.01.356.
22. Karthikeyan M, Nagarajan V. Chloride analysis of sea sand for making concrete. Natl Acad Sci Lett. 2017;40(1):29–31. https://doi.org/10.1007/s40009-016-0493-6.
23. Yang L, Chen M, Liang C, Lu L, Zhao P, Wu F, Xu J, Huang Y. Improvement in the anti-corrosion property of marine concrete using layered double hydroxides and polyvinylpyrrolidone. Appl Clay Sci. 2022;216: 106385. https://doi.org/10.1016/j.clay.2021.106385.
24. Yang B-X, Xie T-Y, Yu Y, Zheng Y, Xu J-J. Mechanical properties and environmental performance of seawater sea-sand self-compacting concrete. Adv Struct Eng. 2022;25(15):3114–36. https://doi.org/10.1177/13694332221119863.
25. Karthikeyan M, Nagarajan V. Study on sea sand as fine aggregate replacement in concrete, 2018; Available: http://hdl.handle.net/10603/233682; Last accessed date: 20-October-2020.
26. Wang Z, Zhao X-L, Xian G, Wu G, Raman RS, Al-Saadi S, Haque A. Long-term durability of basalt-and glass-fibre reinforced polymer (bfrp/gfrp) bars in seawater and sea sand concrete environment. Constr Build Mater. 2017;139:467–89. https://doi.org/10.1016/j.conbuildmat.2017.02.038.
27. Akshaypande. Self-compacting concrete (scc) market professional survey report 2019. Available: http://bit.ly/2Nw5kdr; Last accessed date: 14-January-2021.
28. Cheraghalizadeh R, Akcaoglu T. Utilization of olive waste ash and sea sand powder in self-compacting concrete. Iran J Sci Technol Trans Civ Eng. 2019;43(4):663–72. https://doi.org/10.1007/s40996-018-0224-y.
29. Mao J, Liu Y, Xu J, Wang Q, Lou Y. Desorption behavior and mechanism of chloride ions in fresh concrete mixtures under electromigration. Constr Build Mater. 2023;362: 129680. https://doi.org/10.1016/j.conbuildmat.2022.129680.
30. Xia J, Chen K, Hu S, Chen J, Wu R, Jin W. Experimental and numerical study on the microstructure and chloride ion transport behavior of concrete-to-concrete interface. Constr Build Mater. 2023;367: 130317. https://doi.org/10.1016/j.conbuildmat.2023.130317.

31. Bachtiar E, Rachim F, Makbul R, Tata A, Irfan-Ul-Hassan M, Kırgız MS, Syarif M, Khitab A, Benjeddou O, Kolovos KG, et al. Monitoring of chloride and Friedel's salt, hydration components, and porosity in high-performance concrete. 2022. https://doi.org/10.1016/j.cscm.2022.e01208.
32. IS 456,. Code of practice for the plain and reinforced concrete. India: Bureau of Indian Standards; 2000. p. 2021.
33. *ASTM C642-21, Standard Test Method for Density, Absorption, and Voids in Hardened Concrete*. ASTM International, Available: https://compass.astm.org/document/?contentCode=ASTM Last accessed date: 6-October-2023.
34. J. 206-2010, Technical code for application of sea sand concrete. 2010.
35. IS 650. Specification for Standard Sand for Testing of Cement. New Delhi: Bureau of Indian Standards; 1991. p. 2018.
36. IS 383. Specification for coarse and fine aggregates from natural sources for concrete. India: Bureau of Indian Standards; 2016. p. 2016.
37. Sandhu RK, Siddique R. Strength properties and microstructural analysis of self-compacting concrete incorporating waste foundry sand. Constr Build Mater. 2019;225:371–83. https://doi.org/10.1016/j.conbuildmat.2019.07.216.
38. Gupta N, Siddique R, Belarbi R. Sustainable and greener self-compacting concrete incorporating industrial by-products: a review. J Clean Prod. 2020. https://doi.org/10.1016/j.jclepro.2020.124803.
39. Juenger MC, Siddique R. Recent advances in understanding the role of supplementary cementitious materials in concrete. Cem Concr Res. 2015;78:71–80. https://doi.org/10.1016/j.cemconres.2015.03.018.
40. Griffiths S, Sovacool BK, Del Rio DDF, Foley AM, Bazilian MD, Kim J, Uratani JM. Decarbonizing the cement and concrete industry: a systematic review of socio-technical systems, technological innovations, and policy options. Renew Sustain Energy Rev. 2023;180: 113291. https://doi.org/10.1016/j.rser.2023.113291.
41. Kang S-T. The use of river sand for fine aggregate in uhpc and the effect of its particle size. Adv Concr Constr. 2020;10(5):431. https://doi.org/10.12989/acc.2020.10.5.431.
42. Specification and Guidelines for Self-Compacting Concrete. EFNARC, 2005.
43. Siddique R. Self-compacting concrete: materials, properties and applications. London: Woodhead Publishing; 2019.
44. Dong Z-Q, Wu G, Xu Y-Q. Bond and flexural behavior of sea sand concrete members reinforced with hybrid steel-composite bars pre-subjected to wet-dry cycles. J Compos Constr. 2017;21(2):04016095. https://doi.org/10.1061/(ASCE)CC.1943-5614.0000749.
45. Wang H, Zhang A, Zhang L, Liu J, Han Y, Shu H, Wang J. Study on the influence of compound rust inhibitor on corrosion of steel bars in chloride concrete by electrical parameters. Constr Build Mater. 2020;262: 120763. https://doi.org/10.1016/j.conbuildmat.2020.120763.
46. Bapat JD. Mineral admixtures in cement and concrete. London: Taylor and Francis Group; 2013.
47. Divitkumar R, Ganesh B, Shrestha J, Pandit BP, Chaulagain A, Rawat B. Rheology of sustainable self compacting concrete with triple blend cementitious materials. In: International conference on structural engineering and construction management. Springer, 2021; pp. 905–919. https://doi.org/10.1007/978-3-030-80312-4_77
48. Zou Y, Wu C, Zhang Z, Jiang J, Yu K, Wang X. Investigation on flexural behavior of novel gfrp grid web-concrete hybrid beam. Eng Struct. 2023;278: 115489. https://doi.org/10.1016/j.engstruct.2022.115489.
49. Wu C, He X, Wu W, Ji K. Low cycle fatigue crack propagation and damage evolution of concrete beams reinforced with gfrp bar. Compos Struct. 2023;304: 116312. https://doi.org/10.1016/j.compstruct.2022.116312.
50. Zeng J-J, Liao J, Liang W-F, Guo Y-C, Zhou J-K, Lin J-X, Yan K. Cyclic axial compression behavior of frp-confined seawater sea-sand concrete-filled stainless steel tube stub columns. Front Mater. 2022;9: 872055. https://doi.org/10.3389/fmats.2022.872055.
51. Li S, Guo S, Yao Y, Jin Z, Shi C, Zhu D. The effects of aging in seawater and swssc and strain rate on the tensile performance of gfrp/bfrp composites: a critical review. Constr Build Mater. 2021;282: 122534. https://doi.org/10.1016/j.conbuildmat.2021.122534.
52. Guo Y-C, Ye Y-Y, Lv J-F, Bai Y-L, Zeng J-J, et al. Effective usage of high strength steel tubes: axial compressive behavior of hybrid frp-concrete-steel solid columns. Thin-Walled Struct. 2020;154: 106796. https://doi.org/10.1016/j.tws.2020.106796.
53. Karimipour A, Abad JMN, Fasihihour N. Predicting the load-carrying capacity of gfrp-reinforced concrete columns using ann and evolutionary strategy. Compos Struct. 2021;275: 114470. https://doi.org/10.1016/j.compstruct.2021.114470.
54. Li ZFZXSCAKLG, Xiao BF. Feasibility of glass/basalt fiber reinforced seawater coral sand mortar for 3d printing. Addit Manuf. 2021;37: 101684. https://doi.org/10.1016/j.addma.2020.101684.
55. Doostmohamadi A, Karamloo M, Afzali-Naniz O. Effect of polyolefin macro fibers and handmade gfrp anchorage system on improving the bonding behavior of gfrp bars embedded in self-compacting lightweight concrete. Constr Build Mater. 2020;253: 119230.
56. Zeng J-J, Guo Y-C, Liao J, Shi S-W, Bai Y-L, Zhang L. Behavior of hybrid pet frp confined concrete-filled high-strength steel tube columns under eccentric compression. Case Stud Constr Mater. 2022;16: e00967. https://doi.org/10.1016/j.cscm.2022.e00967.
57. Liu B, Guo J, Zhou J, Wen X, Deng Z, Wang H, Zhang X. The mechanical properties and microstructure of carbon fibers reinforced coral concrete. Constr Build Mater. 2020;249: 118771. https://doi.org/10.1016/j.conbuildmat.2020.118771.
58. Liu M, Cheng X, Li X, Lu TJ. Corrosion behavior of low-cr steel rebars in alkaline solutions with different ph in the presence of chlorides. J Electroanal Chem. 2017;803:40–50.
59. Abbood IS, Aldeen Odaa S, Hasan KF, Jasim MA. Properties evaluation of fiber reinforced polymers and their constituent materials used in structures-a review. Mater Today Proc. 2021;43:1003–8. https://doi.org/10.1016/j.matpr.2020.07.636.
60. Dai J-G, Bai Y-L, Teng J. Behavior and modeling of concrete confined with frp composites of large deformability. J Compos Constr. 2011;15(6):963–73. https://doi.org/10.1061/(ASCE)CC.1943-5614.0000230.
61. Kavya A, Rao AV. Experimental investigation on mechanical properties of concrete with m-sand. Mater Today Proc. 2020;33:663–7. https://doi.org/10.1016/j.matpr.2020.05.774.
62. Gurumoorthy N, Arunachalam K. Durability studies on concrete containing treated used foundry sand. Constr Build Mater. 2019;201:651–61. https://doi.org/10.1016/j.conbuildmat.2019.01.014.
63. Tjaronge MW, Irmawaty R, Adisasmita SA, Amiruddin A, Hartini H. Compressive strength and hydration process of self compacting concrete (scc) mixed with sea water, marine sand and portland composite cement. Adv Mater Res. 2014;935:242–6. https://doi.org/10.4028/www.scientific.net/AMR.935.242.
64. Vafaei D, Hassanli R, Ma X, Duan J, Zhuge Y. Fracture toughness and impact resistance of fiber-reinforced seawater sea-sand concrete. J Mater Civ Eng. 2022;34(5):04022038. https://doi.org/10.1061/(ASCE)MT.1943-5533.0004179.

65. Liao Q, Su Y, Yu J, Yu K. Compression-shear performance and failure criteria of seawater sea-sand engineered cementitious composites with polyethylene fibers. Constr Build Mater. 2022;345: 128386. https://doi.org/10.1016/j.conbuildmat.2022.128386.
66. Page MJ, McKenzie JE, Bossuyt PM, Boutron I, Hoffmann TC, Mulrow CD, Shamseer L, Tetzlaff JM, Akl EA, Brennan SE, et al. The prisma 2020 statement: an updated guideline for reporting systematic reviews. Int J Surg. 2021;88: 105906. https://doi.org/10.1016/j.ijsu.2021.105906.
67. Zhou J, He X, Shen W. Compression behavior of seawater and sea-sand concrete reinforced with fiber and glass fiber-reinforced polymer bars. ACI Struct J, 2020; 117(4)
68. Qi X, Huang Y, Li X, Hu Z, Ying J, Li D. Mechanical properties of sea water sea sand coral concrete modified with different cement and fiber types. J Renew Mater. 2020; 8
69. Zhang M, Du L, Li Z, Xu R. Durability of marine concrete doped with nanoparticles under joint action of cl-erosion and carbonation. Case Stud Constr Mater. 2023;18: e01982. https://doi.org/10.1016/j.cscm.2023.e01982.
70. Li S, Jin Z, Pang B, Li J. Durability performance of an rc beam under real marine all corrosion zones exposure for 7 years. Case Stud Constr Mater. 2022;17: e01516. https://doi.org/10.1016/j.cscm.2022.e01516.
71. IS 516:1959, Method of tests for strength of concrete. Bureau of Indian Standards, India, 2018.
72. Zhao Y, Hu X, Shi C, Zhang Z, Zhu D. A review on seawater sea-sand concrete: mixture proportion, hydration, microstructure and properties. Constr Build Mater. 2021;295: 123602. https://doi.org/10.1016/j.conbuildmat.2021.123602.
73. Sakthieswaran N, Nagendran N. Utilisation of sea sand as partial replacement of fines in resin bonded cement concrete, Revista Ingeniería de Construcción, 2022; 37(3)
74. Safi B, Saidi M, Daoui A, Bellal A, Mechekak A, Toumi K. The use of seashells as a fine aggregate (by sand substitution) in self-compacting mortar (scm). Constr Build Mater. 2015;78:430–8. https://doi.org/10.1016/j.conbuildmat.2015.01.009.
75. Xiao J, Qiang C, Nanni A, Zhang K. Use of sea-sand and seawater in concrete construction: current status and future opportunities. Constr Build Mater. 2017;155:1101–11. https://doi.org/10.1016/j.conbuildmat.2017.08.130.
76. Yin L, Huang Y, Dang Y, Wang Q. Bond of seawater scoria aggregate concrete to stainless reinforcement. J Renew Mater. 2023; 11(1)
77. Li L, Chen X, Chu S, Ouyang Y, Kwan A. Seawater cement paste: effects of seawater and roles of water film thickness and superplasticizer dosage. Constr Build Mater. 2019;229: 116862. https://doi.org/10.1016/j.conbuildmat.2019.116862.
78. Parthasarathy P, Hanif A, Li Z. Early-age properties of cementitious pastes made with seawater. Mater Today Proc. 2022;65:707–14. https://doi.org/10.1016/j.matpr.2022.03.277.
79. Noor NM, Waliyo RA. A systematic literature review on the effect of seawater as a promising material on the physical and mechanical performance of concrete. Int J Sustain Constr Eng Technol. 2021;12(3):236–47.
80. Pati D, Lorusso LN. How to write a systematic review of the literature. Health Environ Res Design J. 2018;11(1):15–30. https://doi.org/10.1177/1937586717747384.
81. MacDonald J. Systematic approaches to a successful literature review. J Can Health Libr Assoc. 2013;34(1):46–7.
82. Vafaei D, Ma X, Hassanli R, Duan J, Zhuge Y. Microstructural and mechanical properties of fiber-reinforced seawater sea-sand concrete under elevated temperatures. J Build Eng. 2022;50: 104140. https://doi.org/10.1016/j.jobe.2022.104140.
83. Kamath V, Renuka A. Deep learning based object detection for resource constrained devices-systematic review, future trends and challenges ahead. Neurocomputing. 2023. https://doi.org/10.1016/j.neucom.2023.02.006.
84. Van Eck N, Waltman L. Software survey Vosviewer a computer program for bibliometric mapping. Scientometrics. 2010;84(2):523–38.
85. Yu H, Zheng J, Lin Q. Strength prediction of seawater sea sand concrete based on artificial neural network in python. Mater Res Express. 2022;9(3): 035201.
86. Kryzhanovskyi V, Avramidou A, Orlowsky J, Spyridis P. Self-compacting high-strength textile-reinforced concrete using sea sand and sea water. Materials. 2023;16(14):4934. https://doi.org/10.3390/ma16144934.
87. Ramachandran VS, Beaudoin JJ. Handbook of analytical techniques in concrete science and technology: principles, techniques and applications. Amsterdam: Elsevier; 2000.
88. Liu J, An R, Jiang Z, Jin H, Zhu J, Liu W, Huang Z, Xing F, Liu J, Fan X, et al. Effects of w/b ratio, fly ash, limestone calcined clay, seawater and sea-sand on workability, mechanical properties, drying shrinkage behavior and micro-structural characteristics of concrete. Constr Build Mater. 2022;321: 126333. https://doi.org/10.1016/j.conbuildmat.2022.126333.
89. Wang D, Gong Q, Yuan Q, Luo S. Review of the properties of fiber-reinforced polymer-reinforced seawater-sea sand concrete. J Mater Civ Eng. 2021;33(10):04021285. https://doi.org/10.1061/(ASCE)MT.1943-5533.0003894.
90. Cheng S, Shui Z, Sun T, Huang Y, Liu K. Effects of seawater and supplementary cementitious materials on the durability and microstructure of lightweight aggregate concrete. Constr Build Mater. 2018;190:1081–90.
91. Saleh S, Mahmood AH, Hamed E, Zhao X-L. The mechanical, transport and chloride binding characteristics of ultra-high-performance concrete utilising seawater, sea sand and scms. Constr Build Mater. 2023;372: 130815. https://doi.org/10.1016/j.conbuildmat.2023.130815.
92. Dang VQ, Ogawa Y, Bui PT, Kawai K. Effects of chloride ions on the durability and mechanical properties of sea sand concrete incorporating supplementary cementitious materials under an accelerated carbonation condition. Constr Build Mater. 2021;274: 122016.
93. Parung H, Tjaronge MW, Djamaluddin R. Compressive strength of marine material mixed concrete. In: IOP conference series: materials science and engineering, 2017; 271, p. 012066. https://dx.doi.org/10.1088/1757-899X/271/1/012066
94. Yang S, Zang C, Xu J, Fan G. Determination of fracture parameters of seawater sea sand concrete based on maximum fracture load. J Mater Civ Eng. 2020;32(1):04019315. https://doi.org/10.1061/(ASCE)MT.1943-5533.0002981.
95. Cao Y, Bao J, Zhang P, Sun Y, Cui Y. A state-of-the-art review on the durability of seawater coral aggregate concrete exposed to marine environment. J Build Eng. 2022. https://doi.org/10.1016/j.jobe.2022.105199.
96. Cai C, Wu Q, Song P, Zhou H, Akbar M, Ma S. Study on diffusion of oxygen in coral concrete under different preloads. Constr Build Mater. 2022;319: 126147. https://doi.org/10.1016/j.conbuildmat.2021.126147.
97. Lu Z, Liu G, Wu Y, Dai M, Jiang M, Xie J. Recycled aggregate seawater-sea sand concrete and its durability after immersion in seawater. J Build Eng. 2023;65: 105780. https://doi.org/10.1016/j.jobe.2022.105780.

98. Li T, Liu X, Zhang J, Shi F, Zhao M, Shen X, Zhu J, Lyu K, Shah SP, Bao T. Effect of air void structure and mechanical properties of high strength fiber reinforced mortar composed with different construction sand species based on x-ct technology. Mech Adv Mater Struct. 2023. https://doi.org/10.1080/15376494.2023.2165743.
99. IS 5816:1999, Method of test splitting tensile strength of concrete. Bureau of Indian Standards, India, 2018.
100. Wang F, Sun Y, Xue X, Wang N, Zhou J, Hua J. Mechanical properties of modified coral aggregate seawater sea-sand concrete: experimental study and constitutive model. Case Stud Constr Mater. 2023;18: e02095. https://doi.org/10.1016/j.cscm.2023.e02095.
101. Ebead U, Lau D, Lollini F, Nanni A, Suraneni P, Yu T. A review of recent advances in the science and technology of seawater-mixed concrete. Cement Concrete Res. 2022. https://doi.org/10.1016/j.cemconres.2021.106666.
102. Li H, Farzadnia N, Shi C. The role of seawater in interaction of slag and silica fume with cement in low water-to-binder ratio pastes at the early age of hydration. Constr Build Mater. 2018;185:508–18.
103. Afshar A, Jahandari S, Rasekh H, Shariati M, Afshar A, Shokrgozar A. Corrosion resistance evaluation of rebars with various primers and coatings in concrete modified with different additives. Constr Build Mater. 2020;262: 120034. https://doi.org/10.1016/j.conbuildmat.2020.120034.
104. Ren J, Wang X, Xu S, Fang Y, Liu W, Luo Q, Han N, Xing F. Effect of polycarboxylate superplasticisers on the fresh properties of cementitious materials mixed with seawater. Constr Build Mater. 2021;289: 123143. https://doi.org/10.1016/j.conbuildmat.2021.123143.
105. Qiao S, Xiong Z, Li Y, Ye Z, He S, Li L, Zeng Y. Mechanical properties of seawater sea-sand concrete exposed to daily temperature variations. Buildings. 2022;12(5):517. https://doi.org/10.3390/buildings12050517.
106. Mansyur M, Permana D. Mechanical behaviour and microstructure characteristic of concrete by using freshwater and seawater. Civil Eng J. 2020;6(6):1195–203.
107. Rahman SK, Al-Ameri R. Marine geopolymer concrete-a hybrid curable self-compacting sustainable concrete for marine applications. Appl Sci. 2022;12(6):3116. https://doi.org/10.3390/app12063116.
108. Li P, Li W, Sun Z, Shen L, Sheng D. Development of sustainable concrete incorporating seawater: a critical review on cement hydration, microstructure and mechanical strength. Cement Concr Compos. 2021;121: 104100. https://doi.org/10.1016/j.cemconcomp.2021.104100.
109. Evangelista L, De Brito J. Durability performance of concrete made with fine recycled concrete aggregates. Cement Concr Compos. 2010;32(1):9–14. https://doi.org/10.1016/j.cemconcomp.2009.09.005.
110. Younis A, Ebead U, Suraneni P, Nanni A. Fresh and hardened properties of seawater-mixed concrete. Construct Build Mater. 2018;190:276–86.
111. Pungercar V, Musso F. Salt as a building material: current status and future opportunities. Plan J.
112. Sang NT, Quan TM, Dang VQ, Ho LS, George RC, et al. Applicability of concrete containing the binary and ternary system of binder materials under natural marine environment. J Appl Sci Eng. 2022;25(5):881–91. https://doi.org/10.6180/jase.202210_25(5).0019.
113. Neville A. Concrete technology. London: Biritish library; 2010.
114. Sun W, Zheng Y, Zhou L, Song J, Bai Y. A study of the bond behavior of frp bars in mpc seawater concrete. Adv Struct Eng. 2021;24(6):1110–23. https://doi.org/10.1177/1369433220956816.
115. Yao J, Chu S. Durability of sustainable marine sediment concrete. Dev Built Environ. 2023;13: 100118. https://doi.org/10.1016/j.dibe.2022.100118.
116. Luan J, Chen X, Ning Y, Shi Z. Beneficial utilization of ultra-fine dredged sand from Yangtze river channel as a concrete material based on the minimum paste theory. Case Stud Constr Mater. 2022;16: e01098. https://doi.org/10.1016/j.cscm.2022.e01098.
117. Chitkeshwar AK, Naktode PL. Concrete with manufactured sand and the effects on the property of durability. Civ Eng Archit. 2022;10(5):1992–9.
118. Zhang M, Zhu X, Shi J, Liu B, He Z, Liang C. Utilization of desert sand in the production of sustainable cement-based materials: a critical review. Constr Build Mater. 2022;327: 127014. https://doi.org/10.1016/j.conbuildmat.2022.127014.
119. Liao T, Huang X, Yuan J, Ren S, Cai H, Chen X. Effects of desert sand substitution on concrete properties using desert sand-doped artificial sand as the fine aggregate. Ceram Silikáty. 2022;66(4):540–54.
120. Verma A, Babu V, Arunachalam S. Influence of acetic acid soaking and mechanical grinding treatment on the properties of treated recycled aggregate concrete. J Mater Cycles Waste Manage. 2022;24(3):877–99.
121. Verma A, Sarath Babu V, Arunachalam S. Influence of mixing approaches on strength and durability properties of treated recycled aggregate concrete. Struct Concrete. 2021;22:E121–42. https://doi.org/10.1002/suco.202000221.
122. Huynh T-P, Ho LS, Van Ho Q. Experimental investigation on the performance of concrete incorporating fine dune sand and ground granulated blast-furnace slag. Constr Build Mater. 2022;347: 128512. https://doi.org/10.1016/j.conbuildmat.2022.128512.
123. Lv M, An X, Bai H, Li P, Zhang J. Influence of the fine aggregate particle packing effects on the paste rheological thresholds of self-compacting concrete. Constr Build Mater. 2023;397: 132379. https://doi.org/10.1016/j.conbuildmat.2023.132379.
124. Benabed B, Kadri E-H, Azzouz L, Kenai S. Properties of self-compacting mortar made with various types of sand. Cement Concr Compos. 2012;34(10):1167–73. https://doi.org/10.1016/j.cemconcomp.2012.07.007.
125. Mehdipour I, Khayat KH. Understanding the role of particle packing characteristics in rheo-physical properties of cementitious suspensions: a literature review. Constr Build Mater. 2018;161:340–53. https://doi.org/10.1016/j.conbuildmat.2017.11.147.
126. Wang H, Zhang A, Zhang L, Liu J, Han Y, Wang J. Research on the influence of carbonation on the content and state of chloride ions and the following corrosion resistance of steel bars in cement paste. Coatings. 2020;10(11):1071. https://doi.org/10.3390/coatings10111071.
127. Sang NT, Quan TM, Nguyen MH, Ho LS, et al. Performances of eco-fine-grained concrete containing saline sand as partial fine aggregate replacement. J Appl Sci Eng. 2021;24(4):527–39. https://doi.org/10.6180/jase.202108_24(4).0009.
128. Chu S, Yao J. A strength model for concrete made with marine dredged sediment. J Clean Prod. 2020;274: 122673. https://doi.org/10.1016/j.jclepro.2020.122673.
129. Tran VM, Nguyen THY, et al. Enhancing the effectiveness of steam curing for cement paste incorporating fly ash based on long-term compressive strength and reaction degree of fly ash. Case Stud Constr Mater. 2022;16: e01146. https://doi.org/10.1016/j.cscm.2022.e01146.
130. Orak M, Sajedi F. Investigating the effect of using three pozzolans separately and in combination on the properties of self-compacting concrete. Adv Nano Res. 2021;11(2):141–55. https://doi.org/10.12989/ANR.2021.11.2.141.

131. Nanni A. The role of cementitious materials in the next decade, 2016. Available: http://www.claisse.info/Proceedings.htm
132. Mazumder EA, Prasad ML. Performance enhancement of fly ash-based self compacting geopolymer concrete using pre-heating technique. Iran J Sci Technol Trans Civ Eng. 2023. https://doi.org/10.1007/s40996-023-01046-5.
133. Golewski G. Comparative measurements of fracture toughgness combined with visual analysis of cracks propagation using the dic technique of concretes based on cement matrix with a highly diversified composition. Theor Appl Fract Mech. 2022;121: 103553. https://doi.org/10.1016/j.tafmec.2022.103553.
134. Li Z, Zhou X, Ma H, Hou D. Advanced concrete technology. New York: Wiley; 2022.
135. Dinakar P, Babu K, Santhanam M. Durability properties of high volume fly ash self compacting concretes. Cement Concr Compos. 2008;30(10):880–6. https://doi.org/10.1016/j.cemconcomp.2008.06.011.
136. Revilla-Cuesta V, Ortega-López V, Skaf M, Manso JM, et al. Deformational behavior of self-compacting concrete containing recycled aggregate, slag cement and green powders under compression and bending: Description and prediction adjustment. J Build Eng. 2022;54: 104611. https://doi.org/10.1016/j.jobe.2022.104611.
137. Phuc DV, Khoa NT, Effect of ground granulated blast furnace slag and fly ash on mechanical properties and sulfate attack resistance of fine-grained concrete using sea sand. In: 2022 7th national scientific conference on applying new technology in green buildings (ATiGB). IEEE, 2022; p. 183–188.
138. Noor NM, Irmawaty R, Rashid MAQ. Experimental study on cement and fine aggregate replacement with coal bottom ash in seawater-mixed concrete. Int J Integr Eng. 2022;14(9):232–9.
139. Yang S, Li L, Sun Z, Wang J, Guo Q, Yang Y. A closed-form fracture model to predict tensile strength and fracture toughness of alkali-activated slag and fly ash blended concrete made by sea sand and recycled coarse aggregate. Constr Build Mater. 2021;300: 123976. https://doi.org/10.1016/j.conbuildmat.2021.123976.
140. Jin H, Li Z, Zhang W, Liu J, Xie R, Tang L, Zhu J. Iodide and chloride ions diffusivity, pore characterization and microstructures of concrete incorporating ground granulated blast furnace slag. J Mater Res Technol. 2022;16:302–21. https://doi.org/10.1016/j.jmrt.2021.11.155.
141. Hosseini SA. Seawater curing effects on the permeability of concrete containing fly ash. Adv Concrete Constr. 2022;14(3):205.
142. Cheng S, Shui Z, Sun T, Yu R, Zhang G, Ding S. Effects of fly ash, blast furnace slag and metakaolin on mechanical properties and durability of coral sand concrete. Appl Clay Sci. 2017;141:111–7.
143. Long W-J, Xie J, Zhang X, Fang Y, Khayat KH. Hydration and microstructure of calcined hydrotalcite activated high-volume fly ash cementitious composite. Cement Concr Compos. 2021;123: 104213. https://doi.org/10.1016/j.cemconcomp.2021.104213.
144. Sun J, Yue L, Xu K, He R, Yao X, Chen M, Cai T, Wang X, Wang Y. Multi-objective optimisation for mortar containing activated waste glass powder. J Market Res. 2022;18:1391–411. https://doi.org/10.1016/j.jmrt.2022.02.123.
145. Mena J, González M, Remesar JC, Lopez M. Developing a very high-strength low-co2 cementitious matrix based on a multi-binder approach for structural lightweight aggregate concrete. Constr Build Mater. 2020;234: 117830. https://doi.org/10.1016/j.conbuildmat.2019.117830.
146. Zhou Y, Wu G, Li L, Guan Z, Guo M, Yang L, Li Z. Experimental investigations on bond behavior between frp bars and advanced sustainable concrete. Polymers. 2022;14(6):1132. https://doi.org/10.3390/polym14061132.
147. Yao Q, Teng X, Lu C, Sun H, Mo J, Chen Z. Influence of accelerated chloride corrosion on mechanical properties of sea sand ecc and damage evaluation method based on nondestructive testing. J Build Eng. 2023;63: 105520. https://doi.org/10.1016/j.jobe.2022.105520.
148. Vafaei D, Hassanli R, Ma X, Duan J, Zhuge Y. Sorptivity and mechanical properties of fiber-reinforced concrete made with seawater and dredged sea-sand. Constr Build Mater. 2021;270: 121436. https://doi.org/10.1016/j.conbuildmat.2020.121436.
149. Su Y, Xiong Z, Hu Z, Zhu W, Zhou K, Wang J, Liu F, Li L. Dynamic bending study of glass fiber reinforced seawater and sea-sand concrete incorporated with expansive agents. Constr Build Mater. 2022;358: 129415. https://doi.org/10.1016/j.conbuildmat.2022.129415.
150. Xiong Z, Zeng Y, Li L, Kwan A, He S. Experimental study on the effects of glass fibres and expansive agent on the bond behaviour of glass/basalt frp bars in seawater sea-sand concrete. Constr Build Mater. 2021;274: 122100. https://doi.org/10.1016/j.conbuildmat.2020.122100.
151. Raut MV. Leverage of high-volume fly ash along with glass fiber for sustainable concrete, 2022. Available: http://www.jresm.org/archive/resm2022.349st1005.html
152. Chen Y, He Q, Liang X, Jiang R, Li H. Experimental investigation on mechanical properties of glass fiber reinforced recycled aggregate concrete under uniaxial cyclic compression. Clean Mater. 2022;6: 100164. https://doi.org/10.1016/j.clema.2022.100164.
153. Gencel O, Nodehi M, Bayraktar OY, Kaplan G, Benli A, Gholampour A, Ozbakkaloglu T. Basalt fiber-reinforced foam concrete containing silica fume: an experimental study. Constr Build Mater. 2022;326: 126861. https://doi.org/10.1016/j.conbuildmat.2022.126861.
154. Soltanzadeh F, Edalat-Behbahani A, Pereira EN. Bond behavior of recycled tyre steel fiber reinforced concrete and basalt fiber-reinforced polymer bars under static and fatigue loading conditions. J Build Eng. 2023;70: 106291. https://doi.org/10.1016/j.jobe.2023.106291.
155. Xie L, Sun X, Yu Z, Zhang J, Li G, Diao M. Experimental study and mechanism analysis of the shear dynamic performance of basalt fiber-reinforced concrete. J Mater Civ Eng. 2023;35(1):04022374. https://doi.org/10.1061/(ASCE)MT.1943-5533.0004549.
156. Abid SR, Abbass AA, Murali G, Al-Sarray ML, Nader IA, Ali SH. Post-high-temperature exposure repeated impact response of steel-fiber-reinforced concrete. Buildings. 2022;12(9):1364. https://doi.org/10.3390/buildings12091364.
157. Lin M, He S, Qiao S, Xiong Z, Qiu Y, Zhang J, Li L. Combined effects of expansive agents and glass fibres on the fracture performance of seawater and sea-sand concrete. J Market Res. 2022;20:1839–59. https://doi.org/10.1016/j.jmrt.2022.08.019.
158. Chen M, Si H, Fan X, Xuan Y, Zhang M. Dynamic compressive behaviour of recycled tyre steel fibre reinforced concrete. Constr Build Mater. 2022;316: 125896. https://doi.org/10.1016/j.conbuildmat.2021.125896.
159. Zhang C, Hao H, Hao Y. Development of double-helix macro bfrp fibers for concrete reinforcement. Mater Struct. 2021;54(4):165. https://doi.org/10.1617/s11527-021-01762-2.
160. Yu F, Li X, Song J, Fang Y, Qin Y, Bu S. Experimental study on flexural capacity of pva fiber-reinforced recycled concrete slabs. Arch Civ Mech Eng. 2021;21:1–23. https://doi.org/10.1007/s43452-021-00314-3.
161. Huang Y, Wu J, Wang Q. Behaviour of sea sand recycled concrete filled steel tube under axial compression. Proc Inst Civ Eng Struct Build. 2020;173(4):302–12. https://doi.org/10.1680/jstbu.18.00125.

162. Thomas J, Ramaswamy A. Mechanical properties of steel fiber-reinforced concrete. J Mater Civ Eng. 2007;19(5):385–92. https://doi.org/10.1061/(ASCE)0899-1561(2007)19:5(385).
163. Zhou L, Zheng Y, Huo L, Ye Y, Wang X, Song G. Fracture behaviors of hvfa-scc mixed with seawater and sea-sand under three-point bending. Adv Struct Eng. 2022;25(4):716–35. https://doi.org/10.1177/13694332211027313.
164. Sayed U, Li H, Dauletbek A, Ali M, Yang D, Lorenzo R, Ashraf M, Feng Z, Wang Z, Xue X. Bamboo stick diameter, volume and aspect ratios effect on the compressive behavior of bamboo sticks reinforced concrete mixed with sea sand and seawater. Constr Build Mater. 2023;369: 130437. https://doi.org/10.1016/j.conbuildmat.2023.130437.
165. Xue X, Wang F, Hua J, Wang N, Huang L, Chen Z, Yao Y. Effects of polyoxymethylene fiber on fresh and hardened properties of seawater sea-sand concrete. Polymers. 2022;14(22):4969. https://doi.org/10.3390/polym14224969.
166. Alabdullh AA, Biswas R, Gudainiyan J, Khan K, Bujbarah AH, Alabdulwahab QA, Amin MN, Iqbal M. Hybrid ensemble model for predicting the strength of frp laminates bonded to the concrete. Polymers. 2022;14(17):3505. https://doi.org/10.3390/polym14173505.
167. Amin MN, Iqbal M, Khan K, Qadir MG, Shalabi FI, Jamal A. Ensemble tree-based approach towards flexural strength prediction of frp reinforced concrete beams. Polymers. 2022;14(7):1303. https://doi.org/10.3390/polym14071303.
168. Liao J, Zeng J-J, Quach W-M, Zhou J-K. Axial compressive behavior and model assessment of frp-confined seawater sea-sand concrete-filled stainless steel tubular stub columns. Compos Struct. 2023;311: 116782. https://doi.org/10.1016/j.compstruct.2023.116782.
169. Zhao C, Wang Z, Zhu Z, Guo Q, Wu X, Zhao R. Research on different types of fiber reinforced concrete in recent years: An overview. Constr Build Mater. 2023;365: 130075. https://doi.org/10.1016/j.conbuildmat.2022.130075.
170. Mirdarsoltany M, Abed F, Homayoonmehr R, Alavi-Nezhad-Khalil-Abad SV. A comprehensive review of the effects of different simulated environmental conditions and hybridization processes on the mechanical behavior of different frp bars. Sustainability. 2022;14(14):8834. https://doi.org/10.3390/su14148834.
171. Zhao X, Rahman MM, D'Antino T, Focacci F, Carloni C. Effect of bonded length on the load response and failure mode of pull-out tests of gfrp bars embedded in concrete. Constr Build Mater. 2022;347: 128425. https://doi.org/10.1016/j.conbuildmat.2022.128425.
172. Başaran B, Kalkan İ, Beycioğlu A, Kasprzyk I. A review on the physical parameters affecting the bond behavior of frp bars embedded in concrete. Polymers. 2022;14(9):1796. https://doi.org/10.3390/polym14091796.
173. Zhou L, Guo S, Zhang Z, Shi C, Jin Z, Zhu D. Mechanical behavior and durability of coral aggregate concrete and bonding performance with fiber-reinforced polymer (frp) bars: A critical review. J Clean Prod. 2021;289: 125652. https://doi.org/10.1016/j.jclepro.2020.125652.
174. Zhao H, Ren T, Remennikov A. Compressive behavior of novel hybrid standing support incorporating fiber-reinforced polymer. In: ARMA US rock mechanics/geomechanics symposium. ARMA, 2020; p. ARMA–2020.
175. Li D, Zhou J, Ou J. Damage, nondestructive evaluation and rehabilitation of frp composite-rc structure: A review. Constr Build Mater. 2021;271: 121551. https://doi.org/10.1016/j.conbuildmat.2020.121551.
176. Wei W, Liu F, Xiong Z, Yang F, Li L, Luo H. Effect of loading rates on bond behaviour between basalt fibre-reinforced polymer bars and concrete. Constr Build Mater. 2020;231: 117138. https://doi.org/10.1016/j.conbuildmat.2019.117138.
177. Deng P, Cong Z, Liu Y, Huang Y, Zhu Q. Effect of dry-wet cycles on bfrp bars and modified ceramsite concrete in marine environments. J Mater Civ Eng. 2022;34(7):04022125. https://doi.org/10.1061/(ASCE)MT.1943-5533.0004273.
178. Reis E, de Azevedo R, Christoforo A, Poggiali F, Bezerra A. Bonding of steel bars in concrete: a systematic review of the literature. Structures. 2023;49:508–19. https://doi.org/10.1016/j.istruc.2023.01.141.
179. Bahnamiri AB, Mohebi ZH, Dehestani M. A bond strength relationship for steel and glass fiber reinforced polymer bars in concrete. Proc Inst Civ Eng Struct Build. 2022;175(8):605–27. https://doi.org/10.1680/jstbu.19.00212.
180. Khalel H, Khan M, Starr A, Khan KA, Muhammad A. Performance of engineered fibre reinforced concrete (efrc) under different load regimes: A review. Constr Build Mater. 2021;306: 124692. https://doi.org/10.1016/j.conbuildmat.2021.124692.
181. Zeng J-J, Zheng Y-W, Liu F, Guo Y-C, Hou C. Behavior of frp ring-confined cfst columns under axial compression. Compos Struct. 2021;257: 113166. https://doi.org/10.1016/j.compstruct.2020.113166.
182. Zeng J-J, Liang S-D, Li Y-L, Guo Y-C, Shan G-Y. Compressive behavior of frp-confined elliptical concrete-filled high-strength steel tube columns. Compos Struct. 2021;266: 113808.
183. Abed MA, Alkurdi Z, Fořt J, Černỳ R, Solyom S. Bond behavior of frp bars in lightweight scc under direct pull-out conditions: experimental and numerical investigation. Materials. 2022;15(10):3555. https://doi.org/10.3390/ma15103555.
184. Shakiba M, Bazli M, Karamloo M, Mortazavi SMR. Bond-slip performance of gfrp and steel reinforced beams under wet-dry and freeze-thaw cycles: the effect of concrete type. Constr Build Mater. 2022;342: 127916. https://doi.org/10.1016/j.conbuildmat.2022.127916.
185. Liu Y, Zhang H-T, Tafsirojjaman T, Dogar AUR, AlAjarmeh O, Yue Q-R, Manalo A. A novel technique to improve the compressive strength and ductility of glass fiber reinforced polymer (gfrp) composite bars. Constr Build Mater. 2022;326: 126782. https://doi.org/10.1016/j.conbuildmat.2022.126782.
186. Hui C, Li Y, Zhou Z, Hai R. Behavior of concrete-filled gfrp tube columns under cyclic axial compression. Constr Build Mater. 2021;294: 123566. https://doi.org/10.1016/j.conbuildmat.2021.123566.
187. Wang X, Zhou L, Liang Y, Zheng Y, Li L, Di B. Study on shear behaviors and damage assessment of circular concrete short columns reinforced with gfrp bars and spiral stirrups. Polymers. 2023;15(3):567. https://doi.org/10.3390/polym15030567.
188. Soares S, Freitas N, Pereira E, Nepomuceno E, Pereira E, Sena-Cruz J. Assessment of gfrp bond behaviour for the design of sustainable reinforced seawater concrete structures. Constr Build Mater. 2020;231: 117277. https://doi.org/10.1016/j.conbuildmat.2019.117277.
189. Zhou L, Zheng Y, Huo L, Ye Y, Chen D, Ma H, Song G. Monitoring of bending stiffness of bfrp reinforced concrete beams using piezoceramic transducer enabled active sensing. Smart Mater Struct. 2020;29: 105012. https://doi.org/10.1088/1361-665X/ab936d.
190. Xiong Z, Deng J, Liu F, Li L, Feng W. Experimental investigation on the behavior of gfrp-rac-steel double-skin tubular columns under axial compression. Thin-Walled Struct. 2018;132:350–61.
191. Abdullah QN, Abdulla AI. Flexural behavior of a box ferrocement beams consisting of self-compacted mortar reinforced by fiber glass mesh and gfrp bars after exposure to high temperatures. J Build Eng. 2023;74: 106917. https://doi.org/10.1016/j.jobe.2023.106917.
192. Małek M, Jackowski M, Łasica W, Kadela M, Wachowski M. Mechanical and material properties of mortar reinforced with glass fiber: an experimental study. Materials. 2021;14(3):698. https://doi.org/10.3390/ma14030698.

193. Xiong Z, He S, Kwan A, Li L, Zeng Y. Compressive behaviour of seawater sea-sand concrete containing glass fibres and expansive agents. Constr Build Mater 292: 123309 (2021)
194. Xiang Z, Zhou J, Niu J. Compressive behavior of cfrp-confined steel fiber-reinforced self-compacting lightweight aggregate concrete in square columns. J Build Eng. 2022;59: 105118. https://doi.org/10.1016/j.jobe.2022.105118.
195. Wang Q, Zhu H. Identification of the bond between ribbed cfrp bars and novel ars anchorage. Constr Build Mater. 2022;327: 126811. https://doi.org/10.1016/j.conbuildmat.2022.126811.
196. Xie J, Liu Y, Qiao Y, Yan J-B. Bond behaviors of ribbed cfrp bars in concrete exposed to low temperatures. Constr Build Mater. 2022;341: 127910. https://doi.org/10.1016/j.conbuildmat.2022.127910.
197. Ji Y, Kim YJ. Durability investigations into cfrp-confined concrete in h2so4. Spec Publ. 2019;331:136–50.
198. Wang X, Ding S, Qiu L, Ashour A, Wang Y, Han B, Ou J. Improving bond of fiber-reinforced polymer bars with concrete through incorporating nanomaterials. Compos B Eng. 2022;239: 109960. https://doi.org/10.1016/j.compositesb.2022.109960.
199. Xiong Z, Zhou K, Ye Z, He S, Li L, Li Y, Zeng Y, Liu F. Bond behavior of basalt fiber reinforced polymer bars in seawater sea-sand concrete exposed to daily temperature variations. Adv Struct Eng. 2022;25(9):2021–39. https://doi.org/10.1177/13694332221098023.
200. Dong Z, Wu G, Zhu H, Wei Y, Zhao X-L, Shao X. Bond and flexural performance of basalt fiber-reinforced polymer bar-reinforced seawater sea sand glass aggregate concrete beams. Adv Struct Eng. 2021;24(15):3359–74. https://doi.org/10.1177/13694332211026228.
201. Pavlović A, Donchev T, Petkova D, Limbachiya M. Short-and long-term prestress losses in basalt frp prestressed concrete beams under sustained loading. J Compos Constr. 2022;26(6):04022069. https://doi.org/10.1061/(ASCE)CC.1943-5614.0001259.
202. Yang J, Guo Y, Tan J, Shen A, Wu H, Li Y, Lyu Z, Wang L. Strength deterioration and crack dilation behavior of bfrc under dynamic fatigue loading. Case Stud Constr Mater. 2022;16: e01051. https://doi.org/10.1016/j.cscm.2022.e01051.
203. Mai G, Li L, Chen X, Xiong Z, Liang J, Zou X, Qiu Y, Qiao S, Liang D, Liu F. Fatigue performance of basalt fibre-reinforced polymer bar-reinforced sea sand concrete slabs. J Market Res. 2023;22:706–27. https://doi.org/10.1016/j.jmrt.2022.11.135.
204. Xiong Z, Lin L, Qiao S, Li L, Li Y, He S, Li Z, Liu F, Chen Y. Axial performance of seawater sea-sand concrete columns reinforced with basalt fibre-reinforced polymer bars under concentric compressive load. J Build Eng. 2022;47: 103828. https://doi.org/10.1016/j.jobe.2021.103828.
205. Motwani P, Rather AI, Laskar A. Transfer stage parameters for concrete beams prestressed with bfrp bars: experimental and finite element studies. Constr Build Mater. 2022;315: 125639. https://doi.org/10.1016/j.conbuildmat.2021.125639.
206. Navya K, Rakesh S. Studies on the effects of basalt fibres on the durability characteristics of high strength self compacting concrete. Mater Today Proc. 2022;60:253–8. https://doi.org/10.1016/j.matpr.2021.12.512.
207. Hua Y, Yin S, Feng L. Bearing behavior and serviceability evaluation of seawater sea-sand concrete beams reinforced with bfrp bars. Constr Build Mater. 2020;243: 118294. https://doi.org/10.1016/j.conbuildmat.2020.118294.
208. Chai LJ, Guo LP, Chen B, Sun PY, Ding C, Liu ZC, Wang LY, Wang YK. Design method of serviceability limit states of bfrp bar reinforced ecological high ductility concrete beam: experimental and theoretical analysis. Structures. 2022;40:855–65. https://doi.org/10.1016/j.istruc.2022.04.065.
209. Zeng J-J, Gao W-Y, Duan Z-J, Bai Y-L, Guo Y-C, Ouyang L-J. Axial compressive behavior of polyethylene terephthalate/carbon frp-confined seawater sea-sand concrete in circular columns. Constr Build Mater. 2020;234: 117383. https://doi.org/10.1016/j.conbuildmat.2019.117383.
210. Ge W-J, Zhu J-W, Ashour A, Yang Z-P, Cai X-N, Yao S, Yan W-H, Cao D-F, Lu W-G. Effect of chloride corrosion on eccentric-compression response of concrete columns reinforced with steel-frp composite bars. J Compos Constr. 2022;26(4):04022042. https://doi.org/10.1061/(ASCE)CC.1943-5614.0001231.
211. Ge W, Chen K, Guan Z, Ashour A, Lu W, Cao D. Eccentric compression behaviour of concrete columns reinforced with steel-frp composite bars. Eng Struct. 2021;238: 112240. https://doi.org/10.1016/j.engstruct.2021.112240.
212. Taha A, Alnahhal W. Bond durability and service life prediction of bfrp bars to steel frc under aggressive environmental conditions. Compos Struct. 2021;269: 114034. https://doi.org/10.1016/j.compstruct.2021.114034.
213. Liu S, Zhou Y, Zheng Q, Zhou J, Jin F, Fan H. Blast responses of concrete beams reinforced with steel-gfrp composite bars. Structures. 2019;22:200–12. https://doi.org/10.1016/j.istruc.2019.08.010.
214. Kurtoğlu AE, Hussein AK, Gülşan ME, Çevik A. Flexural behavior of hdpe tubular beams filled with self-compacting geopolymer concrete. Thin-Walled Struct. 2021;167: 108096. https://doi.org/10.1016/j.tws.2021.108096.
215. Alaneme K, Bodunrin M, et al. Corrosion behavior of alumina reinforced aluminium (6063) metal matrix composites. J Miner Mater Charact Eng. 2011;10(12):1153–65.
216. Amirtharaj J, Mariappan M. Exploring the potential uses of aluminium metal matrix composites (ammcs) as alternatives to steel bar in reinforced concrete (rc) structures-a state of art review. J Build Eng. 2023. https://doi.org/10.1016/j.jobe.2023.108085.
217. Kaufmann J. Evaluation of the combination of desert sand and calcium sulfoaluminate cement for the production of concrete. Constr Build Mater. 2020;243: 118281. https://doi.org/10.1016/j.conbuildmat.2020.118281.
218. Han S, Zhou A, Ou J. Relationships between interfacial behavior and flexural performance of hybrid steel-frp composite bars reinforced seawater sea-sand concrete beams. Compos Struct. 2021;277: 114672. https://doi.org/10.1016/j.compstruct.2021.114672.
219. Yao X, Pei Z, Zheng H, Guan Q, Wang F, Wang S, Ji Y. Review of mechanical and temperature properties of fiber reinforced recycled aggregate concrete. Buildings. 2022;12(8):1224. https://doi.org/10.3390/buildings12081224.
220. Taffese WZ, Nigussie E. Autonomous corrosion assessment of reinforced concrete structures: feasibility study. Sensors. 2020;20(23):6825. https://doi.org/10.3390/s20236825.
221. Taffese WZ, Nigussie E, Isoaho J. Internet of things based durability monitoring and assessment of reinforced concrete structures. Proc Comput Sci. 2019;155:672–9. https://doi.org/10.1016/j.procs.2019.08.096.